HORSESHOE CRAB SPAWNING IN THE DELAWARE BAY – A POTENTIAL RESPONSE TO SEA SURFACE TEMPERATURE

By:

SEAN THATCHER

A thesis submitted to the

School of Graduate Studies

Rutgers, The State University of New Jersey

In partial fulfillment of the requirements

For the degree of

Master of Science

Graduate Program in Geography

Written under the direction of

Richard G. Lathrop

And approved by

_____

_____

_____

New Brunswick, New Jersey

October 2020

ABSTRACT OF THE THESIS

Horseshoe Crab Spawning in the Delaware Bay – A Potential Response to Sea Surface Temperature

By SEAN THATCHER

Thesis Director:

Richard G. Lathrop

The American horseshoe crab *Limulus polyphemus* (HSC) spawns in their greatest densities in the Delaware Bay; however, over-harvests have reduced their population size by 90% in the late 20th century and climate change is degrading their spawning habitat. Because their eggs are an important food source for threatened shorebird species and adjust the timing they spawn due to ocean temperatures efforts were made to understand sea surface temperatures (SSTs) throughout the Bayshore area, patterns of egg cluster abundances and surface densities, identify a SST threshold for peak spawning activity, and use physical characteristics related to specific sites identified as increasing egg abundances. The highest egg abundances – specifically clusters – were in the southern region and decreased northward, while SSTs showed the opposite pattern. Surface egg densities were also the most abundant in the Southern region but are believed to be transported widely within and between regions. The CART analysis identified that the

five-day moving average for SST of 17° C when abundance shifted from pre-peak to post-peak and currently occurs between May 29 and June 5. This temperature threshold was determined to have advanced by several days for all regions and beaches with the Northern region experiencing the most significant advancement, suggesting that a potential does exist for a mismatch to develop if HSCs spawn earlier to match this advancement. Beach nourishment activities will be important for the continued existence of suitable habitat for HSC spawning in the Bayshore area and should focus on increasing the physical parameters that increase cluster abundance such as having sand depth of at least 40 cm and beach width of at least 22 m. As climate change continues to alter the physical habitat in the Bayshore area, continued monitoring of when HSCs are spawning as a response to SST will be important to understand if this mismatch is developing, potentially jeopardizing the recovering red knot population. The MUR dataset is a useful and time and cost-efficient way to monitor SSTs in the Bayshore area for both beaches and regions, allowing it to be implemented in surveying HSC spawning to identify more specific temperature patterns.

Acknowledgements

I would like to thank Dr. Lathrop for all his help with my thesis. Your feedback was consistently constructive and pushed me to grow and learn new skills that will help me in the future. I would also like to thank Dr. Joseph Smith for collecting the horseshoe crab data used in this thesis and data analysis recommendations, without you this would not be possible. I would like to thank Jim Trimble for his help with the data analysis and technological expertise. Dr. Carrie Ferraro saw past my personal limitations and saw the person behind them, without you I would not be here. Lastly, I would like to thank the other members of my committee Dr. Laura Schneider and Dr. Dave Robinson for your feedback and encouragement during my time in the department

I would also like to thank the other graduate students in the Geography Department and C2R2 Program. Our conversations, struggles, successes, and laughs made the arduous process worthwhile. Without all of you I would not have grown to the person I am today by exposing me to new ideas, and concepts from diverse fields. Alana, Natalie, Logan, Rachael, Chris, Jing, Stuti, and everyone else made this a life changing experience – I would not change a moment.

Finally, I would like to thank my family, friends, mentors, and supports for helping me on this journey. Thank you for encouraging me when I needed it most, pushing me when I was tired, listening when I needed to talk, and advising when I was lost. I cannot list all of your names here, my parents, sisters, Mike, Jackie, Jodi, Danny, Sarah, Johnny, Will, Dr. Atchison, Dr. Marshall, and Dr. Alexander all deserve a special mention as I would not be the person I am without all of you help and encouragement.

Table of Contents

List of Tables

List of Tables

Introduction

The main objective of this project is to understand the SST in the Delaware Bay area and how it potentially impacts the spawning behavior of *L. polyphemus,* along with the distribution of their egg densities on beach surfaces and those laid as clusters in burrows. Efforts have been made to understand changes at a high-resolution for individual beaches in the Bayshore area to better understand geographic patterns concerning sea surface temperatures and egg abundances. These efforts are aimed further at using independent variables to relate restoration efforts at individual beaches to better understand their effectiveness, such as beach nourishment activities, towards improving the ecological resilience of HSC spawning habitat.

Research Questions

Three main questions were addressed:

1) Has the temporal pattern of SSTs in near-shore zone of Delaware Bay during the peak spawning season of HSC changed during the 2003 and 2019 time period, utilizing the MUR dataset?
    a. Do SST measurements from MUR correlate well with daily mean *in situ* buoy measurements over this time period?
    b. Do patterns of anomalous SST emerge geographically?
2) What is the SST threshold for spawning activity in the Delaware Bay utilizing the MUR dataset and collected data on HSC surface egg densities, cluster abundances, and other physical variables between 2015 and 2019 using a Classification and Regression Tree Analysis?

a. Do patterns of abundance emerge for HSC egg clusters and surface densities emerge geographically?
b. What are the significance of the variables used deciding the abundance of HSC egg clusters and surface egg densities, along with their individual importance in the model?
c. Is a similar temperature threshold proposed for both surface egg densities and egg clusters?

3) At what date does each individual horseshoe crab spawning beach reach the proposed threshold across the 2003 to 2019 time period, and does a significant trend emerge during this time period at these locations?

Background

Coastal Systems and Climate Change in the Northeast United States

Coastal systems are highly dynamic and susceptible to changes at a variety of spatial and temporal scales due to natural and anthropogenic processes. Locations of high energy due to wind and wave action have assisted in the development of large beach systems composed of dunes, barrier islands, and sandy beaches that are attractive for humans and wildlife species alike (Defeo, et al., 2009; Lazarus, et al., 2016). Low energy coastal systems have assisted in the development of some of the most productive ecosystems such as extensive coastal wetlands and estuaries, along with a variety of geomorphological structures that create diverse macro and micro habitats that are of ecological importance for a variety of species to thrive (Jackson, et al., 2002; Tagliapietra, et al., 2009). Many of these ecosystems have become firmly established over the last 5,000 years as the rate of sea-level rise (SLR) slowed to approximately 2.2 ± 0.8 mm/yr and increased generally in a linear fashion since then (Gehrels, 1994; Miller, et al., 2013). This low rate of SLR has not only benefited coastal ecosystems and the individual species that comprise it, but communities and industry that have developed in these regions due to the abundance of natural resources and access to trade (Nicholls, 2011).

Today the stability of these ecosystems and communities are experiencing changes due to anthropogenic forcing such as through dam development, beach nourishment, and urbanization, but more importantly through climate change due to increasing anthropogenic activities (Spalding, et al., 2014; Lazarus, et al., 2016; Sánchez-Arcilla, et al., 2016; He & Silliman, 2019). As more heat is trapped in the atmosphere it is

radiated down towards the surface increasing ocean temperatures as heat is absorbed and accelerating the rate of SLR through thermal expansion, potentially faster than ecosystems and communities can adapt (Church & White, 2006; Nicholls, 2011; Miller, et al., 2013; Spalding, et al., 2014; Sánchez-Arcilla, et al., 2016; He & Silliman, 2019). Physical changes to the environment including SLR, coastal erosion, and habitat degradation have been identified as stressors to society and ecosystems in the northeastern U.S. by coastal managers that need to be considered in the future for

effective management and policy actions in wake of a changing climate (Smith, et al., 2018).

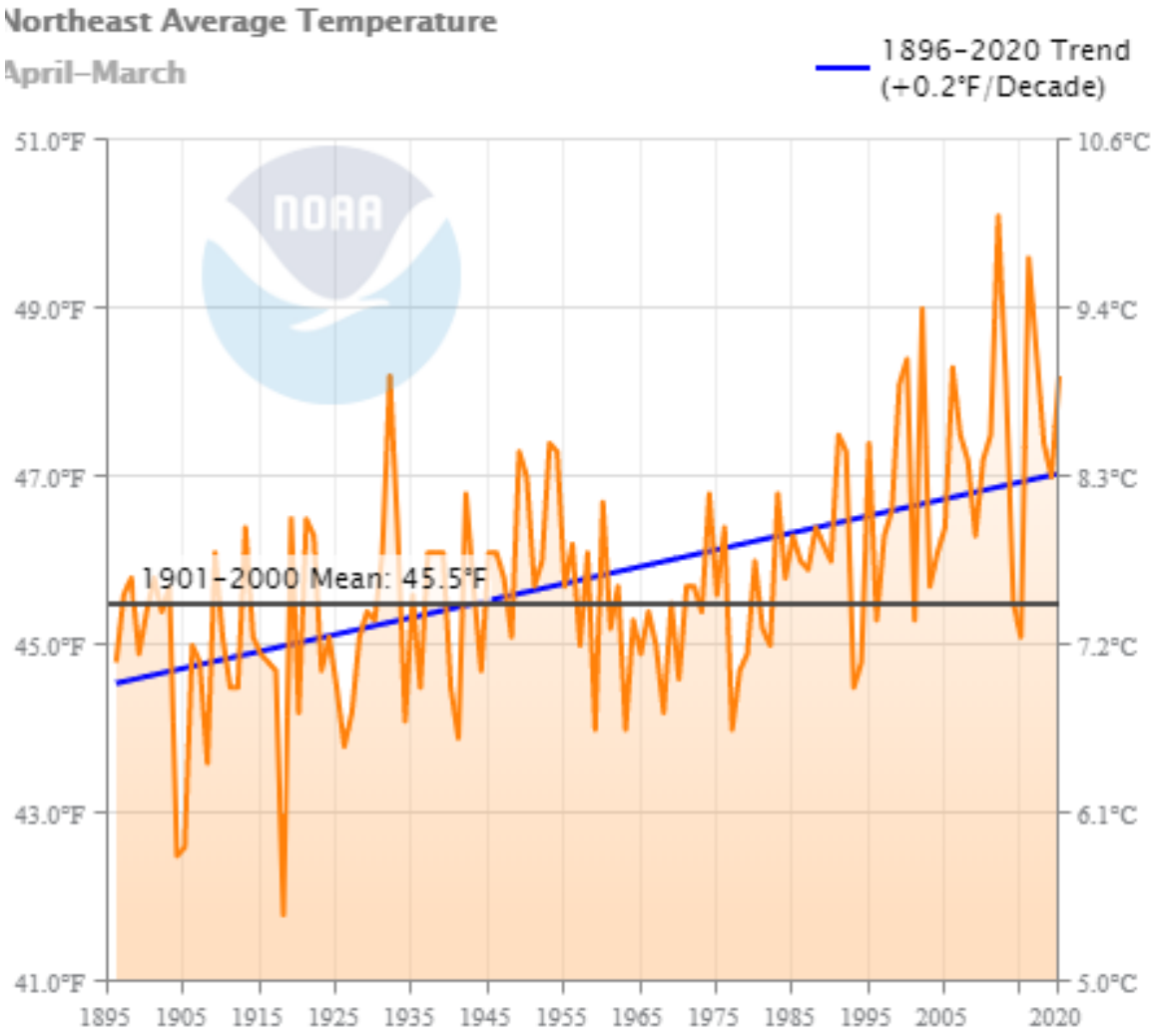

Figure 1: Average air surface temperature baseline determined between 1901 to 2000 shows that there has been approximately a 0.8° C linear increase, with 0.11° C/decade (NOAA, 2020)

Physical changes in coastal ecosystems can be extensive ranging from salinity, sediment amount and type, nutrient loading, SLR, coastal erosion, and habitat degradation (Hale, et al., 2015; Smith, et al., 2018), but changes in the atmosphere and ocean temperatures can create significant changes to individual species or ecosystems at

large (Thomas, et al., 2017; Piao, et al., 2019). In the northeast of the United States reliable records for atmospheric temperatures date back to the late 1800s and show a linear increasing trend of 0.11° C/decade, as seen in Figure 1 (NOAA, 2020). Changes in ocean temperatures, specifically sea surface temperature (SST), differ based upon where you look in the water column, scale, time of year, and the instruments used (Okuro, et al., 2014; Saba, et al., 2016; Thomas, et al., 2017). Thomas *et al.* (2017) found with over 33 years of satellite data that SST have been warming at a rate of approximately 0.3° C/decade in the Mid-Atlantic Bight, with more rapid warming in early and late summer with rates of approximately 1° C/decade. As the rates of warming increase during these time periods SST reach higher temperatures earlier in the year it can encourage some organisms to begin specific biological activities earlier in the year in response to warmer temperatures and are imperative to study in important ecological locations such as the Delaware Bay (Finchman, et al., 2013; Cheng, et al., 2016; Thomas, et al., 2017).

Delaware Bay and the Atlantic Horseshoe Crab

The Delaware Bay Estuary is situated on the eastern seaboard of the United States between the states of New Jersey and Delaware, with Pennsylvania at the most northern inland extent. Delaware Bay is a low energy intertidal estuary with wave heights averaging less than 0.20 m with a maximum mean height of 0.50 m during storm events (Jackson, 1995; Jackson, et al., 2002; Smith, et al., 2011; Jackson, et al., 2020). The low wave energy has allowed for the development of expansive saltmarshes' fringed with the sandy veneer in the mid to northern reaches of the bay, with sandy beaches in the southern reaches as the mouth of the bay to the Atlantic Ocean (Jackson, 1995; Lathrop, et al., 2006; Lathrop, et al., 2013; Partnership of the Delaware Estuary, 2017). The low energy characteristics of the bay in conjunction with a variety of habitats from sandy beaches, coastal wetlands, and intertidal creeks provides ideal habitat for a variety of spawning marine species including Atlantic sturgeon (*Acipenser oxyrinchus oxyrinchus*), Blue crab (*Callinectes sapidus*), Weakfish (*Cynoscion*), and the Atlantic horseshoe crab (*Limulus polyphemus*) to name a few (Partnership of the Delaware Estuary, 2017; Jackson, et al., 2020).

The Atlantic horseshoe crab is approximately 450 million years old and has fondly been given the title of a living fossil as its been little changed since then (Watson III, et al., 2016). The species spends most of its time foraging in the benthos of the Atlantic Ocean, but makes its way to the coastal zone to begin breeding (Sekiguchi & Shuster, 2009; Smith, et al., 2017). *L. polyphemus* can be found spawning over a large geographic area from Maine to the Gulf of Mexico, but the largest numbers are observed in the Delaware Bay (Sekiguchi & Shuster, 2009; Lathrop, et al., 2013; Smith, et al.,

2017). Spawning in the Bayshore area can occur between April through July, but the peak of the spawning activity occurs between May through June depending upon lunar cycles, ocean temperatures, and storm activity (Lathrop, et al., 2006; Smith, et al., 2010; Smith, et al., 2011; Lathrop, et al., 2013; Smith, et al., 2017; Atlantic States Marine Fisheries Commission, 2019).

Although *L. polyphemus* spawn in their greatest densities in this location, their population size has experienced significant decreases historically in the Bayshore area as a source of fertilizer during the 1800's (Breese, 2017). The population began to increase again with the creation of more modern fertilizers, but in recent years population declines are due to anthropogenic stressors from aquaculture, habitat disturbance, and to a limited extent the pharmaceutical industry (Zimmerman, et al., 2016; Breese, 2017; Smith, et al., 2017; Atlantic States Marine Fisheries Commission, 2019). The largest contributor to the recent declines in population was due to their over-harvesting for use as bait in the emerging whelk fishery in the late 1900's (Breese, 2017; Smith, et al., 2017). Because of the importance of *L. polyphemus* eggs being a valuable food resource for migratory and threatened bird species a moratorium was placed on harvesting females in the early 2000's to assist the population in rebounding, but because it takes 8-12 years for juveniles to reach sexual maturity and it is currently unknown the effectiveness of these resource management efforts (Breese, 2017). Despite this factor being unknown, it is believed that the current horseshoe crab population is either stable or increasing gradually at the present time (Smith *et.al.*, 2017).

L. polyphemus prefers low energy coastal environments and have shown a preference to delay spawning to prevent morality from stranding, with wave heights less

than 0.25 m and a periodicity of 2.5 s (Smith, et al., 2002; Jackson, et al., 2020). The Bayshore area exhibits a semi-diurnal micro tidal cycle ranging between 1.6 -1.9 m (Jackson, et al., 2020). Beach morphology and sediment size are important characteristics for beach selection with a preference for coarse grained sediments, low slope angle, and smaller beach width (Jackson, 1995; Smith, et al., 2002; Smith, et al., 2011; Shuster, 2015; Smith, et al., 2017; Jackson, et al., 2020). These site specific characteristics are important to understand beach selection, but water temperature and tidal pressure are widely accepted as important factors for increased HSC activity and spawning synchronization of the species (Smith, et al., 2010; Chabot & Watson, 2010; Smith, et al., 2017; Atlantic States Marine Fisheries Commission, 2019).

L. polyphemus spawn in large groups in the Bayshore area and have been shown that they have synchronized their spawning based upon changes in tidal pressure associated with lunar cycles and typically coincide with high tide as the primary driver of spawning (Chabot & Watson, 2010; Smith, et al., 2017). Horseshoe crabs spawn communally with males clasped to the carapace of a female making their way onto the beach to burrow into the sediment creating a nest in which egg clusters are deposited – exceeding 2,300 eggs on average – with opportunistic satellite males nearby to attempt to fertilize eggs (Smith, et al., 2017). This event can create high surface egg densities on the beach surface, as seen in Figure 2, that have the potential to average several thousand per square meter due to wave action and bioturbation that brings them to the surface from their nests (Jackson, et al., 2020). This signal to initiate spawning is believed to be relatively stable resulting in a predictable signal for horseshoe crabs to begin spawning that is understood by humans and other species, however spawning will be delayed if

suitable water temperatures are not present or occur earlier if ocean temperatures are suitable making it a prime secondary driver to initiate spawning activities in the Bayshore area (Smith, et al., 2002; Smith & Michels, 2006; Chabot & Watson, 2010; Smith, et al., 2010; Watson III, et al., 2016; Cheng, et al., 2016; Smith, et al., 2017).

Figure 2: Image on the beach surface during the 2018 HSC spawning season. The off-green colored sediments are the dense surface egg densities exhumed through bioturbation and wave action located near Fortescue Beach, New Jersey, on May 24.

Water temperatures in the Delaware Bay between May and June are widely believed to be suitable for the spawning of *L. polyphemus* when it reaches 15° C (Smith, et al., 2002; Smith & Michels, 2006; Tucker, et al., 2019), however this is based on

limited spatial data from the Brandywine Shoal, Ship John Shoal, Cape May, or Lewes buoys in the bay maintained by NOAA as seen in Figure 3. These buoys are situated close to the mouth or central areas of the Bay, but do not provide detailed information on temperature in the whole area or close to the coast for long periods of time. Along with the limited spatial coverage, other research suggests that a different suitable temperature threshold may exist and could be different between populations or regions on the eastern seaboard based upon laboratory and *in situ* studies (Chabot & Watson, 2010; Smith, et al., 2010; Watson III, et al., 2016).

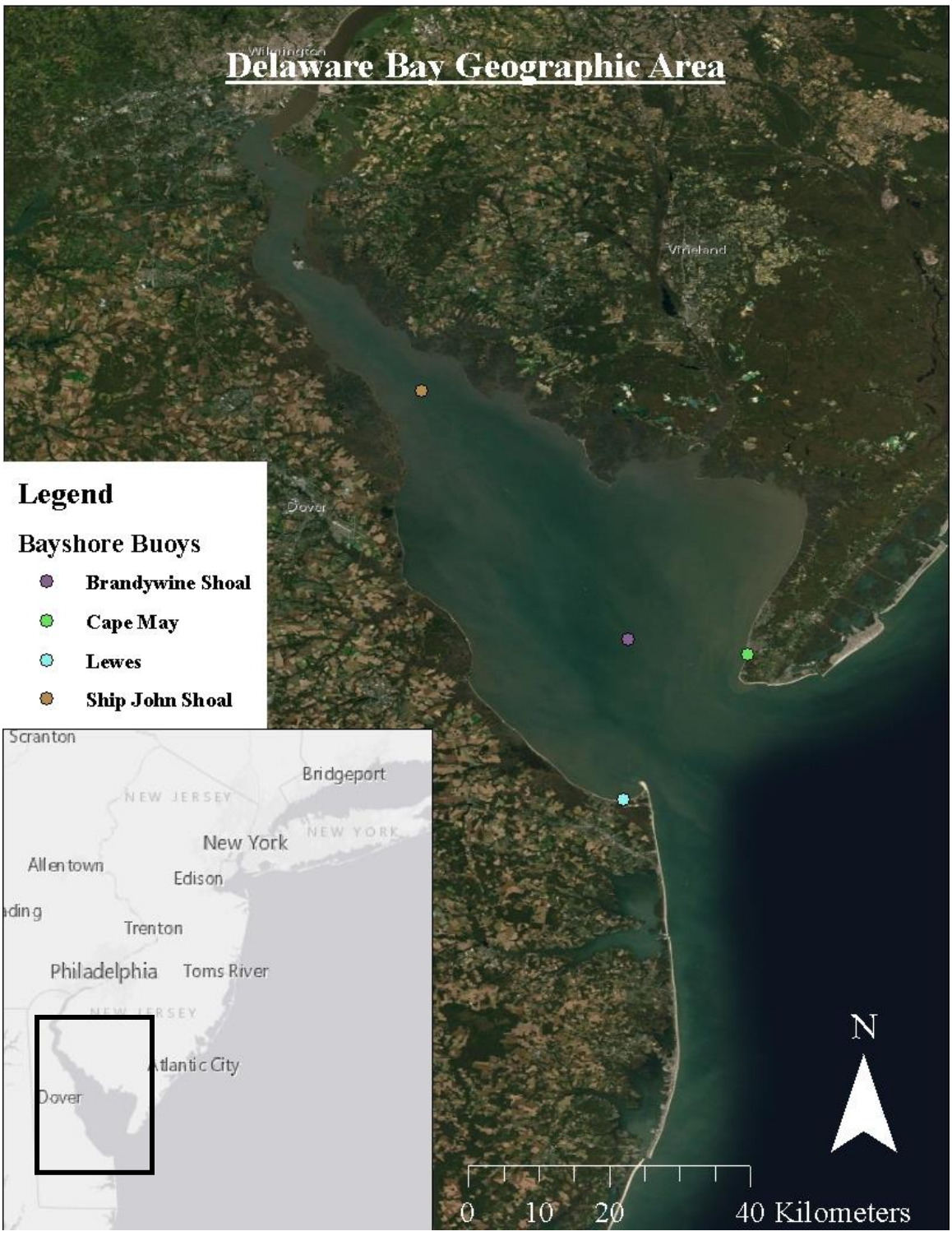

Figure 3: Geographic area of the Delaware Bay and the distribution of buoys within the region from the National Data Buoy Center maintained by NOAA.

Chabot & Watson (2010) found during laboratory manipulation studies that *L. polyphemus* becomes active in the Great Estuary, MA, and may begin activities related to spawning, such as making their way into shallow coastal waters, when water temperatures reached 10°-11° C and began spawning when temperatures reach 17° C. Smith *et al.* (2010) used telemetry data on tagged horseshoe crabs in the Delaware Bay and found similar results on their movements as Chabot & Watson (2010) that they begin to move into shallower water, when mean water temperatures in May range between 13.7°-16.3° C during the years of interest. Watson *et.al.* (2016) used telemetry data with similar methodologies as Smith *et al.* and found that horseshoe crabs in the Great Bay Estuary, MA, became more active and moved into shallower waters as ocean temperatures reached 10°-11° C, then began spawning when ocean temperatures reached 15°-17° C. Although an optimal temperature threshold of 15° C may exist there is no definitive evidence it specifically initiates spawning activity and could be a selection for optimal egg incubation temperature and potentially different for individual populations across its geographic range (French, 1979; Smith & Michels, 2006; Smith, et al., 2010; Watson III, et al., 2016; Smith, et al., 2017).

An important finding conducted by Smith *et al.* (2010) during the spawning seasons of 2004 and 2005 was that for every 1° C of mean daily ocean temperature increase during the May spawning of *L. polyphemus* spawning activity advanced by approximately four days. Similar results were also found in Watson III *et al.* (2016) as ocean temperatures in the Great Bay Estuary, MA, were exceptionally warm in 2012 resulting in spawning activity to begin one month earlier than expected. The advancement of spawning activity earlier in the season could play a key role in

deleteriously influencing the population size and distribution of other species (Smith, et al., 2002; Smith & Michels, 2006; Smith, et al., 2010; Smith, et al., 2017). The high abundance of eggs on the beaches in Delaware Bay attracts thousands of migratory making their way from their southern wintering grounds into the northeast and near-arctic to replenish their energy reserves, but changing when these periods of high egg abundances are present could create an ecological mismatch deleteriously impacting the fecundity of their population in the long term (McGowan, et al., 2011; Zimmerman, et al., 2016; Atlantic States Marine Fisheries Commission, 2019; Tucker, et al., 2019).

Ecological Match/Mismatch Hypothesis

Ecological match/mismatch hypothesis (MMH) was proposed in 1969 by David Cushing as a mechanism to explain how predators time their spawning with periods of high prey abundances in marine systems (Cushing, 1969). MMH is useful for understanding how predatory organisms will synchronize their spawning activities to coincide with a species from a lower trophic level they prey upon that receives their spawning and migration cues from other environmental factors such as temperature (Durant, et al., 2005; Durant, et al., 2007). As the impacts of climate change intensify, temporal shifts in the environmental signals such as temperature can trigger a species to begin reproductive activities earlier in the year. As a result species that receive their cues to begin reproduction or migration from relatively consistent signals, such as photoperiod, could potentially miss these periods of high food abundance and decrease their overall fitness (Durant, et al., 2005; Durant, et al., 2007; Jones & Cresswell, 2010).

The potential for mismatch increases for avian species that travel long distances between their wintering and breeding grounds because the impacts of climate change do

not occur uniformly across the planet, higher latitudes experience a higher degree of warming when compared to lower latitudes for example (Jones & Cresswell, 2010). The work conducted by Jones and Cresswell (2010) showed that the population size of long distance migrant birds are expected to decline because of temporal changes of prey abundances at key stop over locations along their migration routes, changes at their breeding grounds, and delayed signals to begin migration due to minimal temperature changes in their low latitude wintering locations.

One species in particular that is being impacted in this way is the red knot (*Calidris canutus rufa*) that primarily migrates from three known locations in Terra del Fuego in Argentina and Chile, Maranhão in Brazil, and the Southeast in the United States towards the Arctic, but stops in the Delaware Bay during the peak horseshoe crab (HSC) spawning period in May and early June to feed upon the high egg densities and replenish their depleted body mass (McGowan, *et.al.*, 2011). The spring migration poleward of the red knot historically has temporally aligned with the spawning of HSC in the Delaware Bay area, such that it is understood to be the most important stopover location along their migratory route to ensure they have the required body mass to make it to their breeding grounds with enough energy to reproduce (McGowan, et al., 2011). As the population size of spawning horseshoe crabs decreased resulting in lower surface egg densities on Bayshore beaches, significant population declines of the red knot population followed, which led it to become classified as a threatened species in 2015 (Niles, et al., 2009; McGowan, et al., 2011; U.S. Fish and Wildlife Service, 2014; U.S. Fish and Wildlife Service, 2019). As the impacts of anthropogenic climate change intensify understanding how physical changes in the environment, particularly temperature, influence when

periods of high resource abundance emerge at key stopover locations is important for both conservation and resiliency initiatives.

Sea Surface Temperatures – Limitations and Resolution Improvements

Increasing atmospheric temperatures have been well documented since the onset of industrialization (Lüthi *et.al.*, 2008; Solomon *et.al.*, 2009; IPCC, 2019), but increases in surface ocean temperatures has been limited spatially and temporally over large areas due to instrumental and technological limitations (Kent *et.al.*, 2010). Sea surface temperature (SST) is the mean temperature of the top few millimeters to the top few meters of the ocean surface depending upon the methodology used (Fisher & Mustard, 2004; Kent, et al., 2010; Okuro, et al., 2014). The earliest measurements for SST were accomplished by measuring the water temperature in a bucket hoisted from the ocean onto a ship and then measuring the temperature of the water with a thermometer, however was prone to error due to heat loss to the atmosphere (Kent, et al., 2010). More frequent measurements were taken through ships engine room intake pipes in the 1900s used to cool the engines, but were prone to a warming bias due to instrumentational error and poor pipe insulation (Kent, et al., 2010). In the 1970s moored and drifting buoys were introduced providing continuous standardized observations of SST within a 0.1° C of the true value (Kent, et al., 2010).

The long record of SST measurements utilizing the aforementioned methodologies provide a useful dataset to understand variations over long periods of time, but does not provide high temporal and spatial resolution as data collection was not consistent or occurred over a limited geographic area (Kent, et al., 2010). In 1993 remote

sensing technologies began recording global SST with a 25 km spatial resolution (Kent, et al., 2010; Okuro, et al., 2014), however this still proved to be to coarse of a resolution to be applied to understanding SST changes near the coastal zone (Fisher & Mustard, 2004). Other satellite platforms such as Landsat and MODIS can measure SST with a resolution of 30 m and 250 m respectively and require corrective algorithms to improve their accuracy, but they also make these measurements using infrared sensors and are easily obscured by cloud cover and have limited temporal coverage (Fisher & Mustard, 2004; Haines, et al., 2007; Okuro, et al., 2014; Chin, et al., 2017).

A new dataset from NASA Jet Propulsion Lab called the Multiscale Ultra-high Resolution (MUR) SST has been created that takes in a multitude of datasets that measures SST and provides a 1 km spatial resolution (Chin, et al., 2017). This dataset blends measurements from buoys and vessels, with data collected from satellites including but not limited to MODIS and AVHRR to create a daily SST snapshot of the planet from 2003 to the present by utilizing a gridless mesh to interpolate temperature (Chin, et al., 2014; Chin, et al., 2017). The MUR dataset opens up new possibilities to examine the spatial and temporal dynamics of SST, and in particular near-shore SST, in much greater detail. Understanding changes in SST in the Delaware Bay coastal regions will help to determine when temperatures in the coastal zone are appropriate for horseshoe crab reproduction (Smith & Michels, 2006; Chabot & Watson, 2010; Cheng, et al., 2016; Smith, et al., 2017). This information will inform the long-term protection and development of policies aimed at HSC population conservation and promote a more resilient Delaware Bay ecosystem.

Resilience – An Ecological Perspective

The concept of resilience has a long history dating back to its Latin roots in ancient Rome, and has been applied to many different fields such as disaster risk analysis, engineering, and human psychology to describe how a system or person can 'bounce back' after a disturbance (Alexander, 2013). Resilience as used here to describe the ability of an ecological system to return to a state of equilibrium after a disturbance occurs was originally proposed by Holling in 1973. Holling describes resilience as the property of the ecological system to absorb changes within state variables – such as temperature – and continue to persist into the future (Holling, 1973). Although an ecological system may be resilient because of its ability to absorb disturbances, as the state variables of a system continue to change due to the impacts associated with climate change, it could cause a system to rebound into a new equilibrium state (Gunderson, 2000). Likewise an ecosystem may return to its previous state, but the biological community or biodiversity will not be the same or as high as its original state prior to the disturbance that created the change to occur (Chazdon, 2008). As the physical parameters that govern the composition and distribution of ecosystems change due to climate change and urbanization processes, it is important to keep in mind that changes in these systems could lead to a variety of regime shifts – the change of one ecosystem into another – in coastal regions (Ernstson, et al., 2010). As this process continues it can change the abundance, distributions, and types of ecosystems and resources that are usually found in these areas, making our current strategies of managing coastal resources obsolete if the spatial distributions of important ecosystems continue to change threatening the resilience of species that depend upon them.

In the Delaware Bay efforts have been made to protect organisms that are important to sustain migratory species and restore degraded habitats within the estuary to improve the overall resilience of these ecological communities. Since the early 2000's in the Bay area restrictions have been placed on HSC harvests to encourage population stabilization efforts due to significant declines associated with the species being used as bait in the fishing industry, with a complete moratorium on the harvest of females on the New Jersey side of the Bay since 2008 (Breese, 2017). Although the ban was initially enacted to assist in stabilizing the population size of the horseshoe crabs reproducing in the Bayshore area, it remains in place today because of the subsequent decline in the population size of the migratory red knot that depends upon high quantities of horseshoe crab eggs to complete their spring migration (Zimmerman, et al., 2016; Breese, 2017). The decline in the red knot population was so substantial at the end of the 20th and early 21st century that in 2015 the species was federally recognized as threatened, providing additional protections to defend against human disturbance and horseshoe crab harvests (U.S. Fish and Wildlife Service, 2019). Despite these types of protection for individual species under the Endangered Species Act in the case of the threatened red knot to increase the resilience of the species and that of its primary food source, climate change remains a primary threat to the ecological resilience of the estuary throughout the remainder of the 21st century.

Methodology

Horseshoe Crab Sampling Methodology

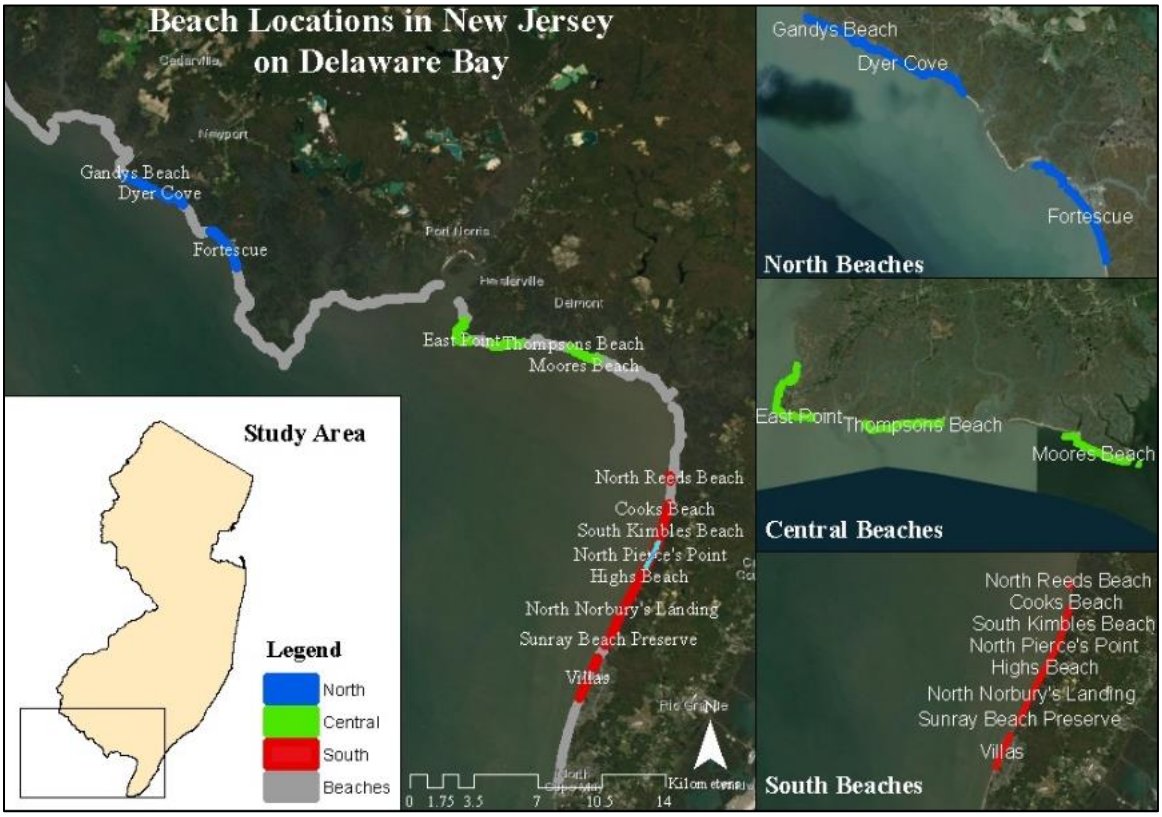

Figure 4: Geographic area of HSC egg cluster and surface egg densities beach sampling locations in the Delaware Bay.

The HSC egg cluster and surface density data used for this project was provided by Smith and closely followed sampling methodologies outlined by Smith *et al.* (2020) along transects at 14 beaches between 2015-2019 as seen in Table 1. Beach selection for this project was determined by choosing the beaches that account for a majority of the spawning activity, a combination of beaches that have and have not been restored recently, and correspond to locations identified as optimal or suitable habitat for spawning horseshoe crabs by Lathrop *et.al.* (2013). Sampling did not occur every year in each of these 14 locations, but the years sampling did occur at each location can also be

observed in Table 2. These beaches were also grouped into three distinct geographic areas corresponding to their location in the Bayshore area, specifically Northern, Central, and Southern groups observed in Figure 4 and Table 1, to make comparisons on abundance and SST spatially to answer questions 3a and 3b.

Beach Groupings	2015	2016	2017	2018	2019
Gandy's Beach	X	X	X	X	X
Dyers Beach		X	X	X	X
Fortescue	X	X	X	X	X
East Point	X	X	X		
Thompsons	X	X		X	X
Moore's Beach	X	X	X	X	X
North Reeds Beach	X	X	X	X	X
Cooks Beach	X	X	X	X	X
South Kimble's	X	X	X	X	X
North Pierce Point	X	X		X	X
Highs Beach	X	X	X	X	X
North Norbury		X	X	X	X
Sunray Beach Preserve	X	X	X	X	X
Villas	X	X	X		X

Table 1: Table that displays the beaches selected to collect data on horseshoe crab surface egg densities and the years samples were collected at these locations for the years between 2015 to 2019 between May and July. Colors correspond to the three geographic regions – Blue in the Northern, Green in the Central, and Red in the Southern.

Surface egg density samples were collected weekly between May and June along 9 m transects between 2015 to 2018 and intermittently in 2019. 9 surface samples at each sampling transect were collected in a 5.7 cm diameter at a depth of 5 cm, placed in plastic bags, and sorted in the lab to separate eggs from the remaining sand. During the separation process the number of eggs collected were counted using a click counter to keep track of the total number of eggs in each sample. The counted number of eggs were rescaled to represent surface eggs per m^2 for each of the sampling transects to represent the surface egg densities on the sampled beaches between May and June. Once the surface egg densities were determined the dataset was imported into a GIS environment

and spatially joined to the individual sampling sites they were collected from. This data was further summarized by date to identify the weekly mean surface egg densities at each location between 2015 to 2019 and classified as pre-peak, peak, and post-peak for the spawning period that year based upon when the maximum density was observed.

HSC egg clusters were also sampled along 5-10 transects at the same beaches depending upon the size of individual beaches. Sampling of HSC clusters began the second week of May and continued until the second week of July throughout 2015-2019. Along these transects 9 20 cm^3 holes were dug with egg clusters of at least 2.5 cm wide in at least one dimension being counted as a single cluster. The HSC egg cluster data was also imported into a GIS environment and spatially joined to their sampling locations and summarized by date to determine the average number of clusters per transect at each beach. Like the surface egg density data clusters were also classified as pre-peak, peak, and post-peak for the spawning period that year based upon when the maximum density was observed.

Sea Surface Temperatures

Week Number	Date Range
1	4/25 to 5/1
2	5/2 to 5/8
3	5/9 to 5/15
4	5/16 to 5/22
5	5/23 to 5/29
6	5/30 to 6/5
7	6/6 to 6/12
8	6/13 to 6/19
9	6/20 to 6/26
10	6/27 to 7/3
11	7/4 to 7/10
12	7/11 to 7/17
13	7/18 to 7/24
14	7/25 to 7/31

Table 2: The weekly breakdown for how yearly and total baselines were created to determine SST anomalies utilizing the MUR dataset.

SST data from MUR was obtained from NASA's Jet Propulsion Lab between April 25 to July 31 for the years between 2003 and 2019 and from 4/25 to 7/3 in 2020. Data from the Cape May, NJ, buoy (44009) was obtained from the National Buoy Center from NOAA also between April 25 to July 31, but extended between the years 1997 to 2019. Data from this buoy was obtained hourly, but only the nighttime temperatures were aggregated together to allow them to be comparable with the MUR dataset. The purpose of extending the year range was to determine if the observed trends in the MUR dataset are comparable to the *in situ* observations and if these trends began prior to the inception of the MUR dataset as mentioned in question 1a. This also assisted in corroborating the accuracy of SST measurements in the Bayshore area to ensure that the two datasets located close to each other geographically displayed similar patterns over time. It is important to note that the two datasets were similar but not identical because the buoy recorded SST measurements approximately 0.6 m below the water surface, while the MUR dataset includes satellite measurements that traditionally measured the top few millimeters and other *in situ* observations at various depths (Chin, et al., 2017).

The MUR dataset was imported into a GIS platform and was used to compile weekly mean SST baseline rasters utilizing the day ranges – 14 weeks total – between 2003-2019 and 10 weeks total in 2020 as observed in Table 2. Weeks were chosen to detect anomalies instead of days because SSTs can exhibit significant variation between individual days, providing a more suitable determination of what typical SSTs were to detect significant anomalies. The baseline rasters were then used to compare weekly baseline rasters for each individual year to determine the presence of statistically significant warmer or colder anomalies throughout the Bayshore area. The anomaly

rasters were used to understand how anomalous SST has potentially changed throughout the Bayshore area, if specific geographic regions of anomalous SST were occurring during the HSC spawning season – as mentioned in question 1b – and if anomalous temperatures have impacted the timing of HSC egg abundances during the years of 2015 to 2019 – as mentioned in question 3a.

Due to the high spatial resolution of the MUR dataset for SST a heavy emphasis was placed on determining SSTs for specific locations in the Delaware Bay. A 3 km buffer was applied to every beach in the Bayshore area to construct a high resolution dataset for the daily mean near-shore SST from April 25 to July 31 between 2003 and 2019 – 53 in total – with a subset if these locations being used to understand HSC spawning behavior in significant detail. A 3 km buffer was decided upon to ensure that enough pixels containing values for SST were available to determine the daily mean, while pixels within each buffer zone that represented the land surface were ignored from this analysis. The daily mean SST between the years of the MUR dataset at these locations were then used to compute a daily baseline to determine how SST has varied at the daily level for individual beaches during the spawning season. This information was used to determine the SST during the day sampling occurred at each location and the SST prior to the sampled spawning activity with a 5 day moving average which were variables used to assist answering questions 3a and 3b, along with comparing SST between the 14 individual HSC sampling sites geographically which was important to understand geographic patterns concerning SST as mentioned in question 1b.

Physical Parameters

Physical characteristics besides SST were also measured by Smith et al. (2020) at individual beaches, including the sand depth until peat or mud in cm, beach width in m, Julian day, and the number of days since the new or full moon – as seen in Table 3. Because HSC shows preference for beaches with sand depth greater or equal to 40 cm, this variable was used to understand if it played a role with cluster abundance and surface egg densities. Beach width was also considered as it has been noted that beach width plays a role in surface egg abundance and may influence spawning behavior if it is smaller as it may be related to lower wave height (Smith, et al., 2011). Wave heights were not considered in this analysis because of its low spatial resolution being in the Bayshore area and not at the individual beach level. Three geographic regions – northern, central, and south – were also used to categorize the location of each beach to understand how abundance for surface egg densities and clusters changed between different locations in the bay, along with if it impacted spawning behaviors. A five-day moving average of SST was also determined for each beach to provide the average SST prior to sampling to better understand temperature conditions prior to the sampling since HSC activity has been observed to increase in the Bayshore area when it reaches 13.7°-16.3° C (Smith, et al., 2010). Lastly the number of days since the new and full moon during the sampling day was determined because tidal pressure is believed to be one of the predominant factors to synchronize HSC spawning activity for the species throughout the entirety of its geographic area (Cheng, et al., 2016; Smith, et al., 2017; Atlantic States Marine Fisheries Commission, 2019).

Table 3: Summary table on the dependent and independent variables in the CART analysis with the sample sizes and sources.

Cluster Physical Parameters				
Variable	*Variable Type*	*Analysis*	*Sample Size*	*Source*
Clusters	Dependent	Regression	676	(Smith, et al., 2020)
Julian Day	Dependent	Classification	676	----------
Class	Dependent	Classification	3	----------
SST	Independent	Both	490	MUR
Five-day SST Average	Independent	Both	676	Derived from MUR
Lunar Phase	Independent	Both	676	https://www.moonpage.com/
Region	Independent	Both	3	----------
Sand Depth	Independent	Both	649	(Smith, et al., 2020)
Beach Width	Independent	Both	579	(Smith, et al., 2020)
Surface Egg Density Physical Parameters				
Variable	*Variable*	*Analysis*	*Sample Size*	*Source*
Surface Egg Density	Dependent	Regression	366	(Smith, et al., 2020)
Julian Day	Dependent	Classification	400	----------
SST	Independent	Both	400	MUR
Five-day SST Average	Independent	Both	382	Derived from MUR
Lunar Phase	Independent	Both	400	https://www.moonpage.com/
Region	Independent	Both	3	----------
Sand Depth	Independent	Both	220	(Smith, et al., 2020)
Beach Width	Independent	Both	334	(Smith, et al., 2020)

Threshold Detection – Classification and Regression Tree Analysis

The physical parameter variables discussed above along with cluster abundance, surface egg density, and SSTs were used in a Classification and Regression Tree (CART) to identify the important variables that influence spawning on beaches using surface egg density and clusters that influence abundance and identify a spawning temperature threshold to answer questions 2a and 2b. The data collected to determine a temperature threshold and variables important for spawning to be initiated and abundance were a combination of both categorical and numerical data, and includes missing variables making many statistical methods impractical. CART grows decision trees from the top

down beginning with a root node and based upon if the dependent variable is either categorical or numerical is classification or regression, respectively. Independent variables can consist of both types of data to determine how to split the data in the best possible way utilizing recursive binary partitioning. This methodology of growing decision trees utilizes each of the independent variables to determine how to split the data to decrease the uncertainty of improperly classifying the data into a specified category in the case of a classification tree, or by reducing the sum of squares error in a regression tree. In both cases the trees grown are typically large and overfit the data used to train the model, requiring the trees to be pruned prior to their use on the test dataset to determine the model's accuracy.

The data inputted for both surface egg density and egg clusters was split using 67% as training data for the model's development and the remaining 33% as test data to use on the trained model to determine accuracy. For the classification tree the trained model was created to identify if the data collected was prior to, at, or after the peak spawning period for that given year using the five-day SST moving average, the SST during the day of sampling, geographic region, and the number of days since the new or full moon for the data collected between 2015 and 2019 as independent variables. A second model was also created with the Julian Day, replacing the SST during the day of sampling, and removing the five-day moving average, because the SST and day are highly correlated – since temperatures increase between the dates selected. Model accuracy was then determined by using the testing data for surface egg density and egg clusters in a validation matrix on correctly and incorrectly classified categories.

The same training and testing data as the classification was used when growing the regression trees. In this instance the dependent variable was average clusters per transects of the log average surface egg density, with the SST during the day of sampling, five-day moving average for SST, sand depth, beach width, region, and days since the new or full moon as independent variables for the data collected between 2015 and 2019. The model was then pruned by selecting the optimal subtree with the lowest by utilizing the lowest value of the cost complexity parameter, a value that possesses the lowest cross validation error and reduces the tree size to increase its predictive accuracy. The model accuracy was then determined using the RMSE.

Lastly the daily mean SST for the 14 HSC spawning beaches was used to determine when the Julian day of the determined threshold from the CART analysis occurred between 2003-2019 to characterize whether this date has advanced or retreated both for geographic regions and specific beaches. Because the date when SST is suitable for spawning to begin varies temporally based on climatological and meteorological factors beyond the scope of this study, it serves as a proxy for when HSC may begin spawning in this location since it has been identified as a primary secondary driver (Smith & Michels, 2006; Watson III, et al., 2016; Smith, et al., 2017). If the advancement is significant it could deleteriously impact the value of the Bayshore area as a stopover for migratory shorebirds, potentially decreasing the resilience of a suite of shorebird species that depend on HSC eggs as key energy resource (McGowan, et al., 2011; Zimmerman, et al., 2016).

Results

HSC Clusters

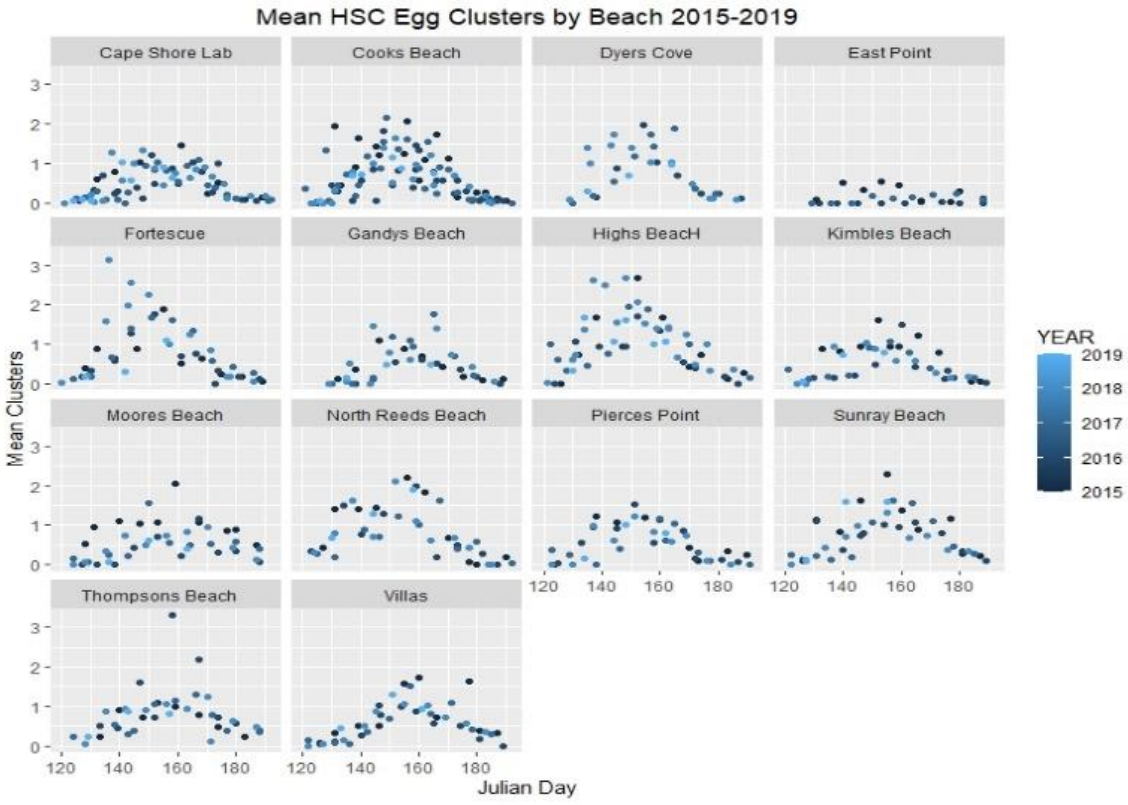

Figure 5: The distribution of mean cluster abundance per transect on individual beaches between 2015 to 2019. Sampling reveals a normal distribution at most beaches related to Julian Day.

The distribution of clusters, observed in Figure 5, have a normal distribution related to the Julian Day between 2015 to 2019 during the spawning season. The distribution suggests that the beginning, peak, and approximate end of the HSC spawning season was captured during these years when aggregated together. Although the entirety of the spawning season was captured, not all beaches equally hosted the same mean cluster abundance per transect or the high temporal resolution of sapling. Cooks Beach, Highs Beach, and Sunray Beach Preserve are all situated in the southern geographic

region and possess high mean cluster abundances per transect, while others in the southern geographic area such as Cape Shore Lab, Kimbles Beach, and Villas all exhibit moderate cluster abundances when compared to the aforementioned locations. This pattern is also present in other geographic regions such as the Central Bayshore area. East Point has the lowest mean cluster abundance per transect out of the observed locations, while Moores Beach and Thompsons Beach have similar distributions in clusters during this time period.

Summary Statistics HSC Egg Cluster 2015-2019 by Geographic Region															
	Year 2015			**Year 2016**			**Year 2017**			**Year 2018**			**Year 2019**		
Region	*N*	*C*	*S*	*N*	*C*	*S*	*N*	*C*	*S*	*N*	*C*	*S*	*N*	*C*	*S*
Mean	0.54	0.58	0.76	0.56	0.60	0.51	0.71	0.50	0.61	0.84	0.55	0.62	0.51	0.50	0.78
Standard Error	0.13	0.07	0.10	0.14	0.23	0.06	0.18	0.09	0.07	0.17	0.11	0.09	0.15	0.13	0.10
Standard Deviation	0.40	0.26	0.55	0.53	0.87	0.38	0.60	0.37	0.46	0.64	0.38	0.49	0.36	0.32	0.42
Range	1.30	0.93	1.73	1.96	3.31	1.31	1.59	1.25	1.54	1.90	1.07	1.68	0.92	0.80	1.25
Minimum	0.09	0.22	0.00	0.00	0.00	0.00	0.06	0.04	0.04	0.02	0.02	0.00	0.17	0.06	0.06
Maximum	1.38	1.15	1.73	1.96	3.31	1.31	1.65	1.29	1.58	1.92	1.09	1.68	1.09	0.86	1.31
Peak Day	151	155	154	156	164	154	160	165	156	141	170	151	156	147	151
Count	10	15	31	15	15	39	11	18	40	14	11	30	6	6	18

Table 4: Summary statistics for HSC egg clusters by geographic regions in the Delaware Bay spawning season from 2015 to 2019.

Patterns concerning cluster abundance per transect do emerge geographically, as seen in Figure 6. Beaches situated in the Southern region of the Bayshore area were observed to have a higher number of mean clusters per transect in all years compared to the other regions – except for 2017 observed in Table 3. Those located in the Northern region of the Bayshore area were expected to show a lower number of mean clusters per transect compared to those in the Central region, however between 2015 to 2019 they were higher comparatively – with exceptions in 2015 and 2016.

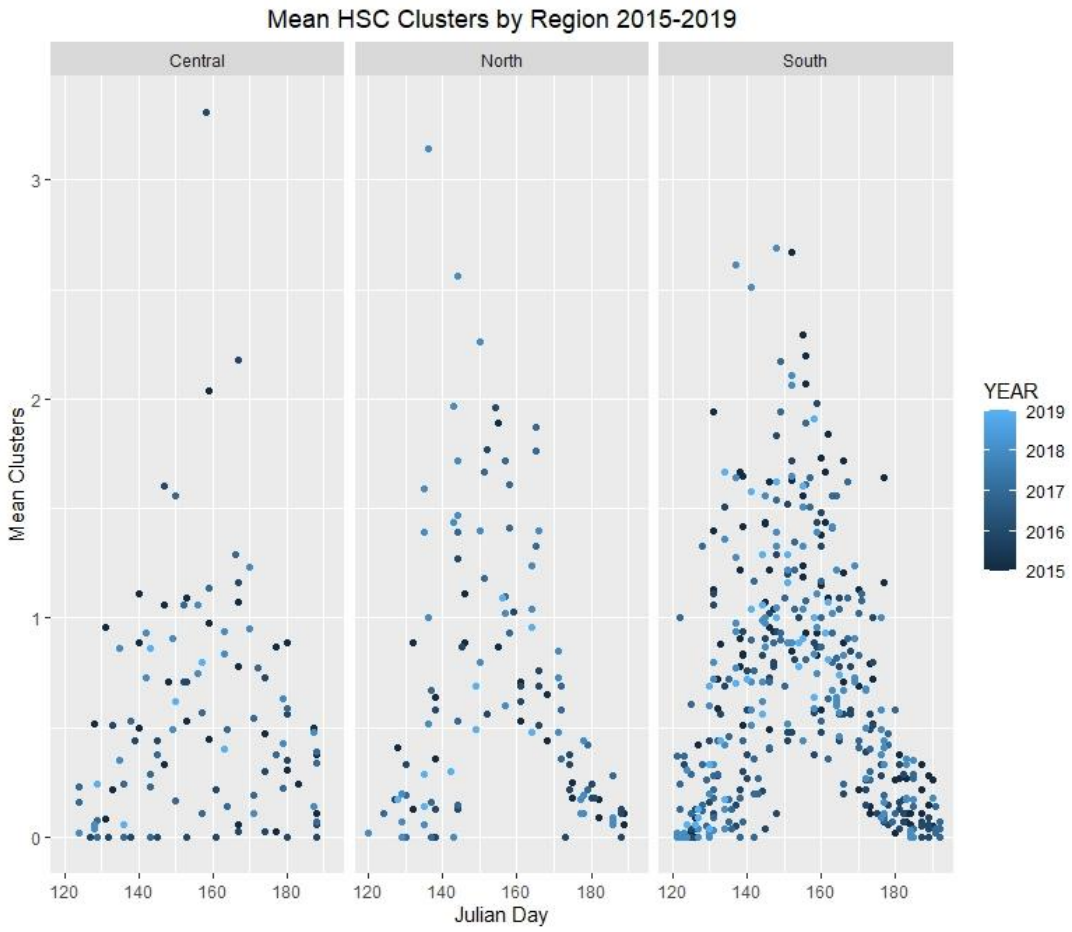

Figure 6: The aggregated distribution of mean cluster abundance per transect by geographic region from 2015 to 2019. Like the results in individual beaches, the cluster abundances by geographic region display a normal distribution.

HSC Surface Egg Densities

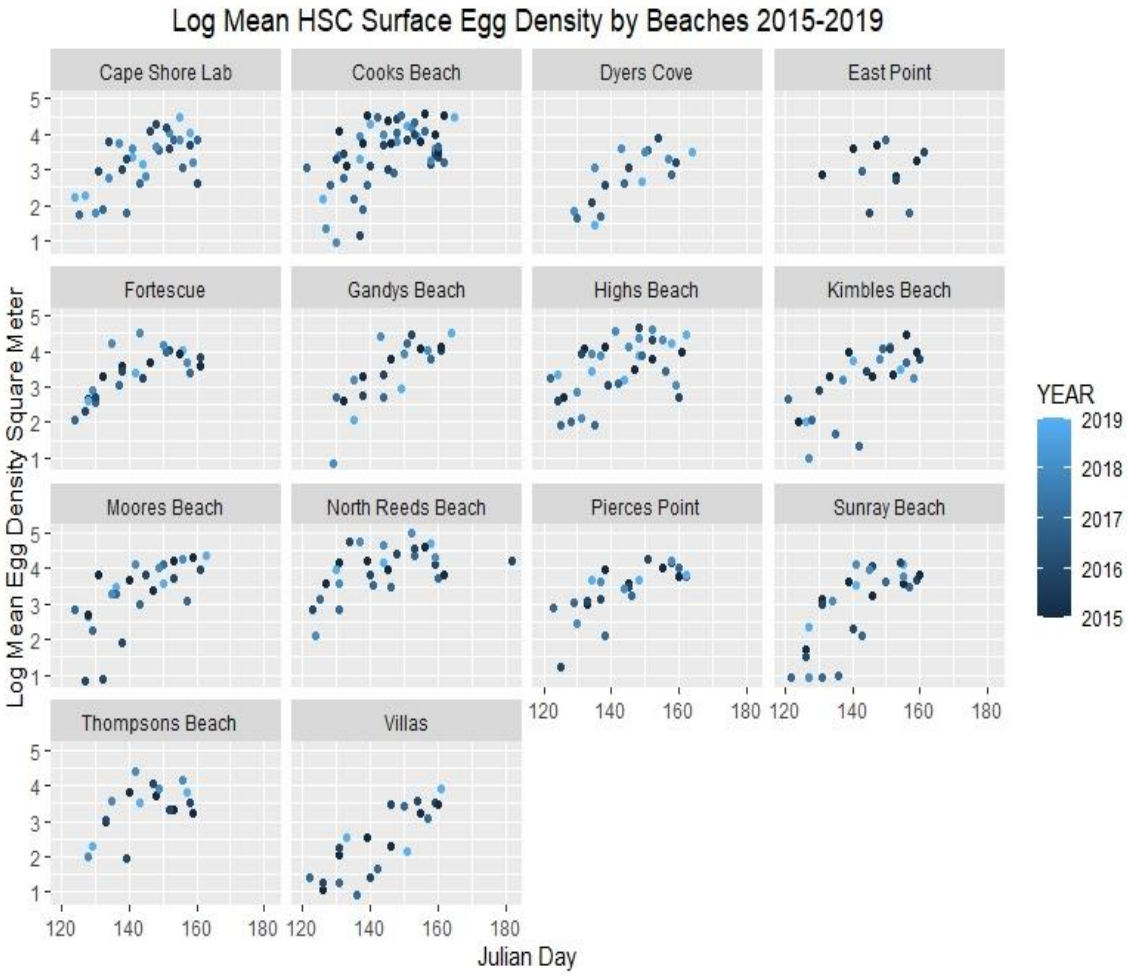

Figure 7: The distribution of the log means surface egg density in m^2. Sampling shows that high surface egg densities do exist, however the peak abundance of surface egg density may not have captured due to early cessation of sampling during the spawning seasons between 2015 to 2019.

Unlike the distributions for HSC clusters by beaches in Figure 5, the distribution of surface egg densities do not share the same pattern observed in Figure 7. Sampling of HSC surface egg densities show a general increase in surface egg densities from the beginning of the sampling period in early May but was cut short in early June. Despite this limitation in data collection, it does clearly show that surface egg densities can easily

exceed 10,000 m^2 in many locations – including East Point which had low mean clusters per transect.

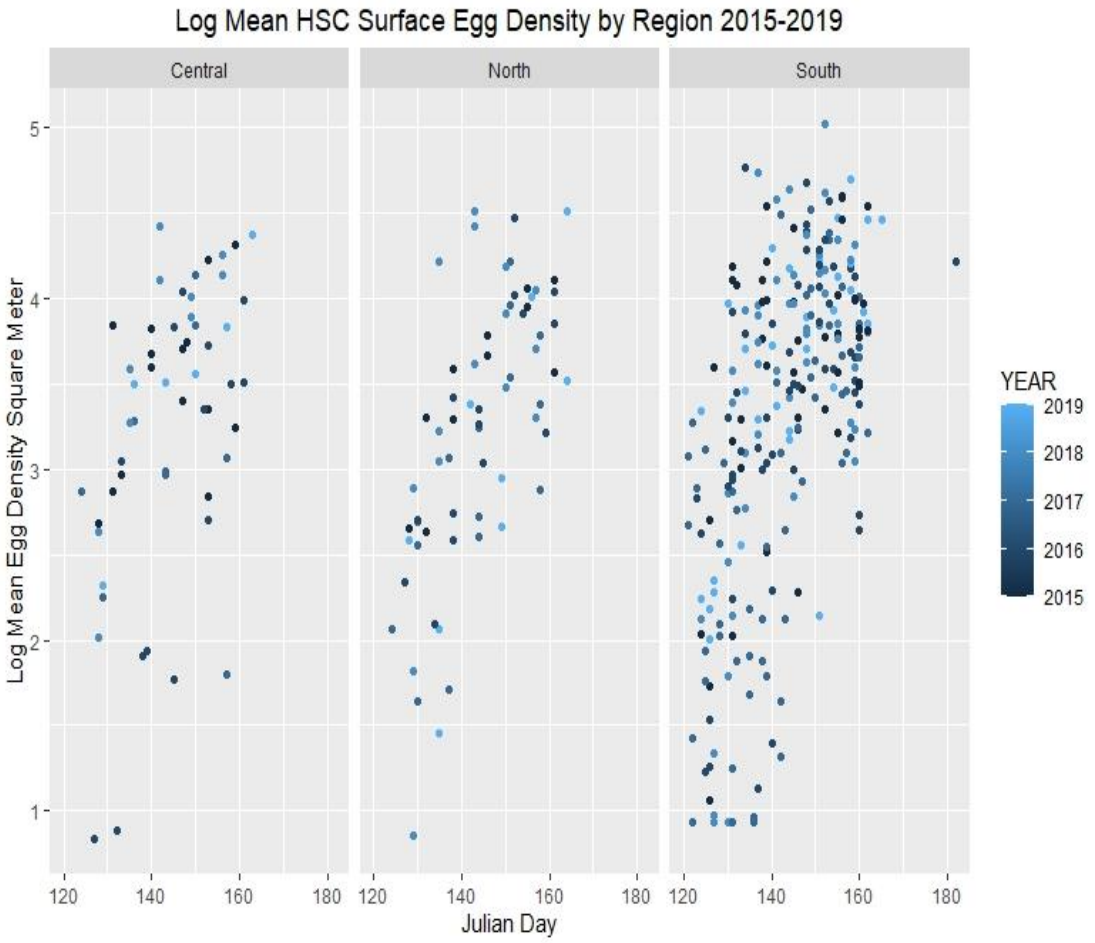

Figure 8: Distribution of log mean surface egg densities per m^2 based upon geographic region. Despite the limited sampling after early June between 2015 to 2019, egg densities in all locations can exceed 10,000 m^2 with more than 100,000 m^2 in rare cases. Densities in the southern region were higher, with similar abundances observed in the North and Central regions.

Surface egg densities by geographic region, observed in Figure 8, clearly show the abrupt break in sampling after early June in all three geographic regions, however insights can be made concerning the abundance of surface egg densities. Surface egg densities regularly exceed 10,000 m^2 in all three regions, however the highest densities are observed in the Southern region – as seen in Figure 8 and Table 4. HSC surface egg

densities are similar in the Northern and Central groupings, however more eggs were observed in the Northern region in 2015 and 2016. Comparing surface egg densities to cluster abundances shows that clusters increase gradually throughout the spawning season, however surface egg densities can increase rapidly throughout the spawning season by several magnitudes in a matter of days – particularly in the Southern region.

	Summary Statistics HSC Surface Egg Densities 2015-2019 by Geographic Region														
	Year 2015			**Year 2016**			**Year 2017**			**Year 2018**			**Year 2019**		
Region	*N*	*C*	*S*	*N*	*C*	*S*	*N*	*C*	*S*	*N*	*C*	*S*	*N*	*C*	*S*
Mean	3.44	3.38	3.55	3.17	2.66	3.28	2.81	2.97	2.84	3.42	3.63	3.38	3.09	3.52	3.52
Standard Error	0.22	0.13	0.16	0.22	0.33	0.17	0.29	0.26	0.17	0.41	0.36	0.24	0.36	0.27	0.17
Standard Deviation	0.53	0.37	0.69	0.71	1.11	0.84	0.71	0.62	0.84	0.91	0.80	0.94	0.88	0.67	0.70
Range	1.36	1.06	2.72	2.16	3.20	3.22	1.85	1.74	3.24	2.33	1.94	3.38	2.26	2.05	2.37
Minimum	2.65	2.68	1.83	2.09	0.84	1.23	2.06	2.25	0.95	1.86	2.33	1.08	1.76	2.32	2.10
Maximum	4.01	3.74	4.55	4.25	4.04	4.45	3.91	3.99	4.19	4.18	4.27	4.46	4.02	4.37	4.46
Peak Day	158	149	153	152	156	153	151	150	155	143	149	151	161	160	156
Count	6	8	18	10	11	25	6	6	25	5	5	15	6	6	18

Table 5: Summary statistics on HSC surface egg densities during the 2015-2019 spawning season in the Delaware Bay for geographic regions.

SST Weekly Anomalies

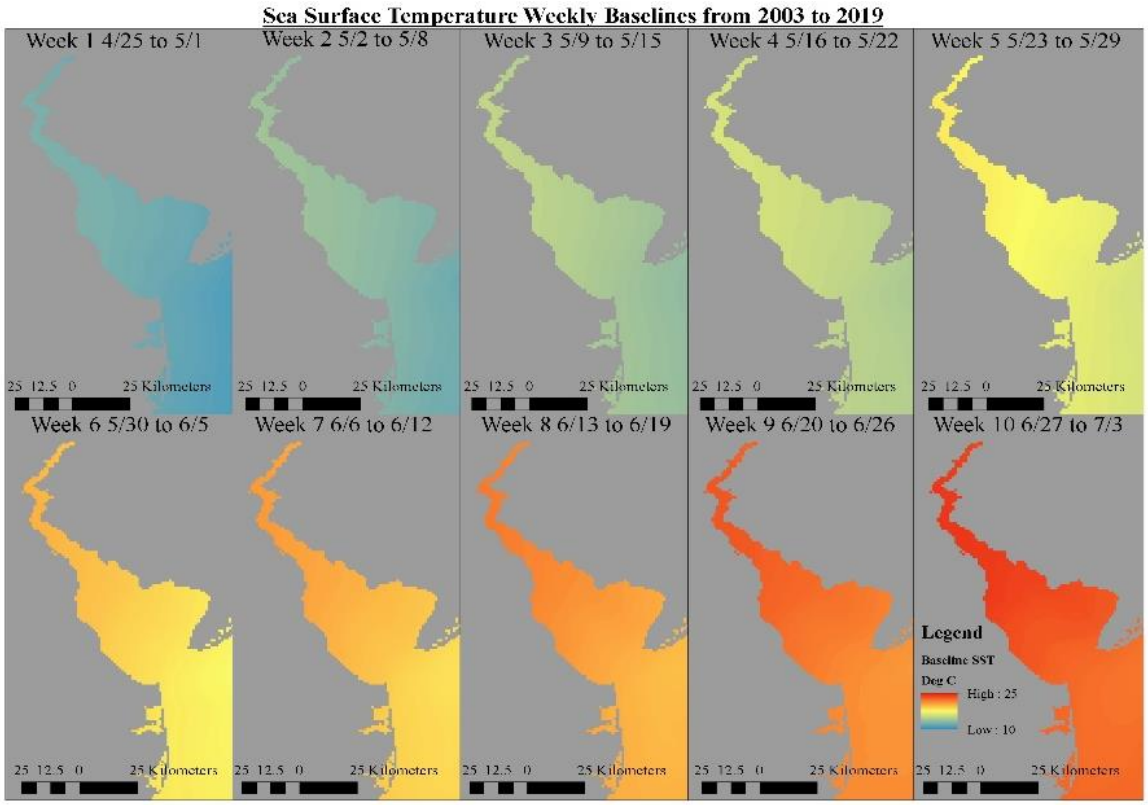

Figure 9: Weekly observations of baseline SST comprised of daily observations for each individual week between the years of interest. As temperatures increase between Weeks 1 through 10 SSTs increases as they move from mid spring to early summer. SSTs are observed to increase more rapidly in the Northern region of the Bayshore area and decrease with increasing proximity to the ocean.

Weekly baseline SST composed of the daily SST observations from the MUR dataset can be observed in Figure 9. SSTs increase throughout the geographic area as the seasons change from mid-spring to early summer. SSTs increase more rapidly in the northern area of the Delaware Bay and more slowly with decreasing proximity to the ocean. This increase is likely due to the shallower water that warms up more quickly than the deeper water closer to the ocean. However, by Week 10 the SST in the area is fairly homogenous, despite warmer SST being present in the Northern areas.

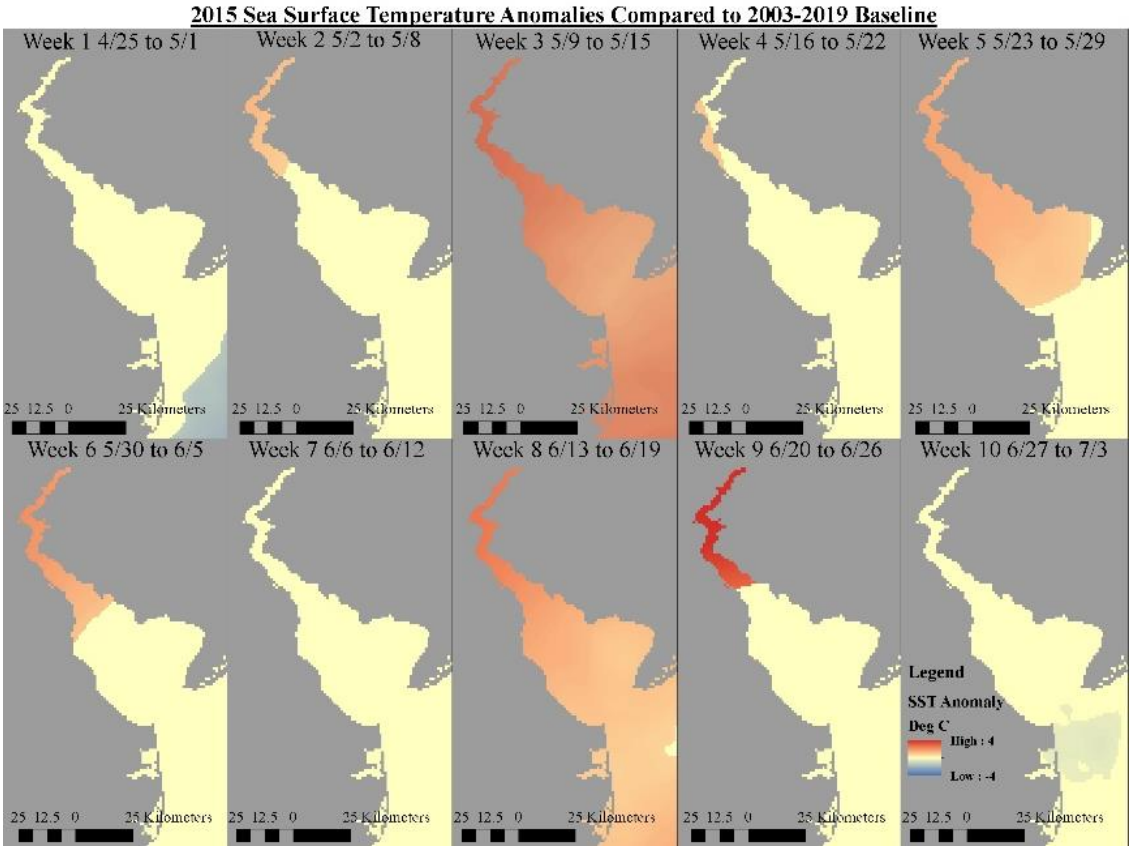

Figure 10: Weekly SST anomalies for 2015 in the Delaware Bay area compared to the baseline SST observed in Figure 7. Beige represents no statistically significant anomaly, warmer colors as statistically significant higher SSTs, and cooler colors as statistically significant lower SSTs.

These baselines were further used to compare to the weekly baselines for each individual year between 2003 to 2020, however only SST anomalies between 2015 to 2020 are reported here. SST anomalies for 2015, observed in Figure 10, showed that colder anomalies did not emerge at the spawning beaches. However warmer SST anomalies between 1° to 1.5° C were observed in Weeks 3, 5, and 7, along with higher anomalies exceeding 2.5° C were observed in the Northern region in Week 9.

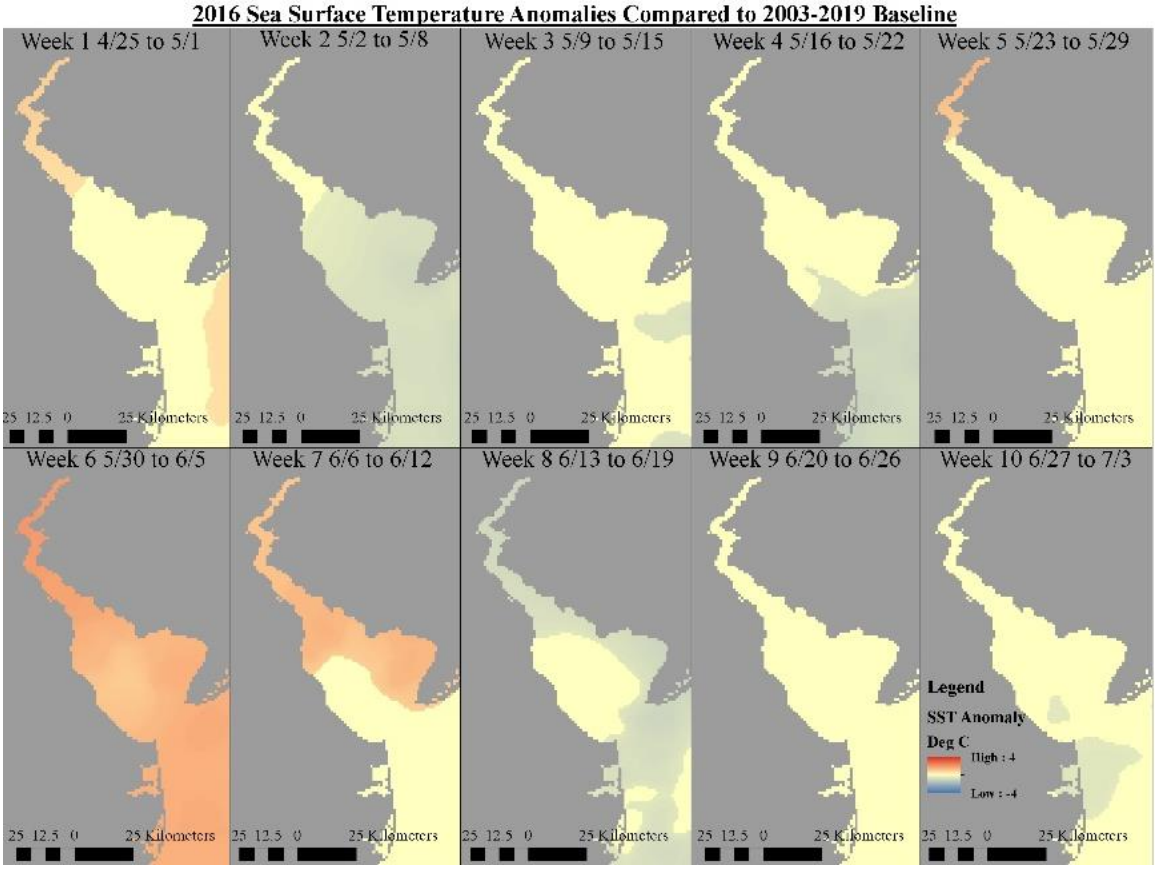

Figure 11: Weekly SST anomalies for 2016 in the Delaware Bay area compared to the baseline SST observed in Figure 7. Beige represents no statistically significant anomaly, warmer colors as statistically significant higher SSTs, and cooler colors as statistically significant lower SSTs.

2016 SSTs showed more variation in anomalous temperatures than the previous year, as observed in Figure 11. Although warmer SSTs were observed in Weeks 6 and 7 throughout the Bayshore area with higher anomalous SSTs in the Northern region in Weeks 1 and 5, cooler temperatures predominated in the other Weeks – with the exception of Weeks 3, 4, 9 and 10 that showed little to no anomalous observations.

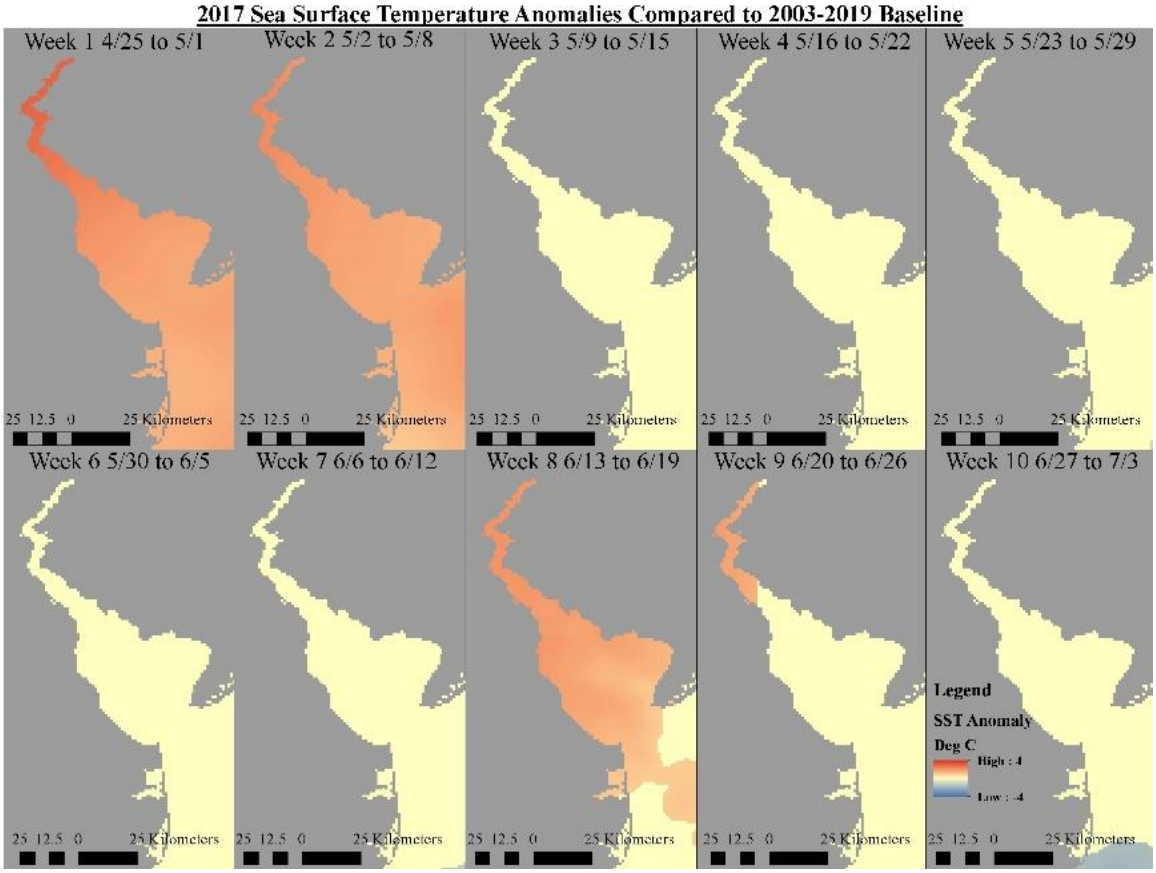

Figure 12: Weekly SST anomalies for 2017 in the Delaware Bay area compared to the baseline SST observed in Figure 7. Beige represents no statistically significant anomaly, warmer colors as statistically significant higher SSTs, and cooler colors as statistically significant lower SSTs.

As in 2015, no cooler anomalous SST were detected in 2017 – as observed in Figure 12. Warmer SSTs were observed in the entire Bayshore area during Weeks 1, 2, and 8 between 1° to 1.5° C, with higher anomalous SSTs in the Northern region in Week 9. The remaining Weeks showed no statistically anomalous SSTs in 2017, suggesting that SSTs in this particular year were typical compared to the baseline temperatures for most of the Weeks in 2017.

2018 anomalous SSTs – observed in Figure 13 – showed only Week 1 exhibited statistically significant cooler temperatures, however this was only observed in the center

and Delaware side of the Bayshore area, and potentially did not influence the beaches of interest on the New Jersey side of the Bay. Warmer anomalous temperatures were observed in Weeks 4 and 6, however like Week 1 they only impacted the center and Delaware side of the Bay and may not have influenced beaches in New Jersey. Significantly warmer SSTs were observed in the Bayshore area during Weeks 2, 3, 5, and 10 between 0.5° to approximately 2° C, while no anomalous temperatures were detected between Weeks 7 through 9.

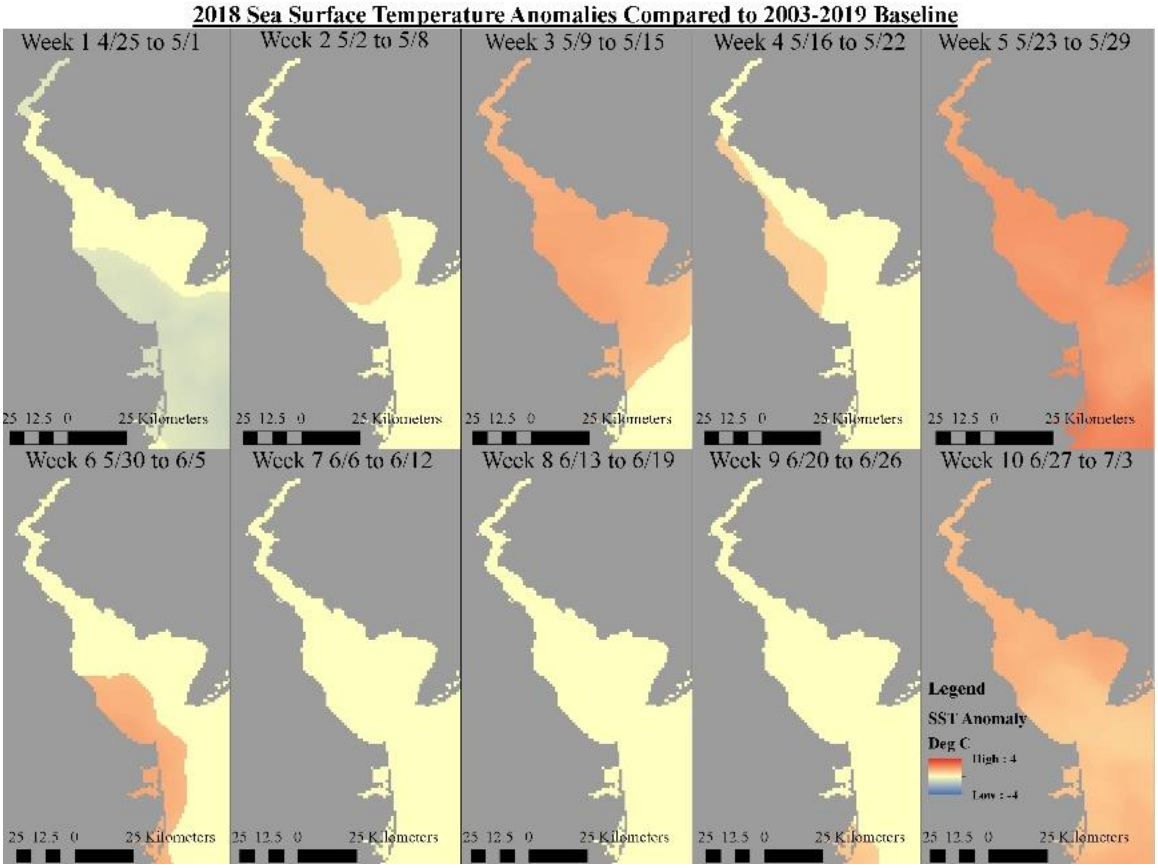

Figure 13: Weekly SST anomalies for 2018 in the Delaware Bay area compared to the baseline SST observed in Figure 7. Beige represents no statistically significant anomaly, warmer colors as statistically significant higher SSTs, and cooler colors as statistically significant lower SSTs.

SSTs for 2019, observed in Figure 14, experienced no observations of cold anomalies between the observed Weeks – except for the Northern region in Week 8. This is distinctly different than the other years that have data collected concerning HSC surface egg densities and clusters. Statistically significant warmer anomalies were of a lower magnitude in Weeks 1, 2, 4, 7, and 9 ranging between 0.5° to 1.5° C. In Week 2 the observed higher SST anomalies most likely had similar influences on location on the New Jersey Bayshore beaches due to their detection of the Delaware side of the Bay, making it similar to Week 3 with no anomalous SST. Weeks 5, 6, and 10 exhibited the highest anomalous SSTs ranging between 1° to 3° C.

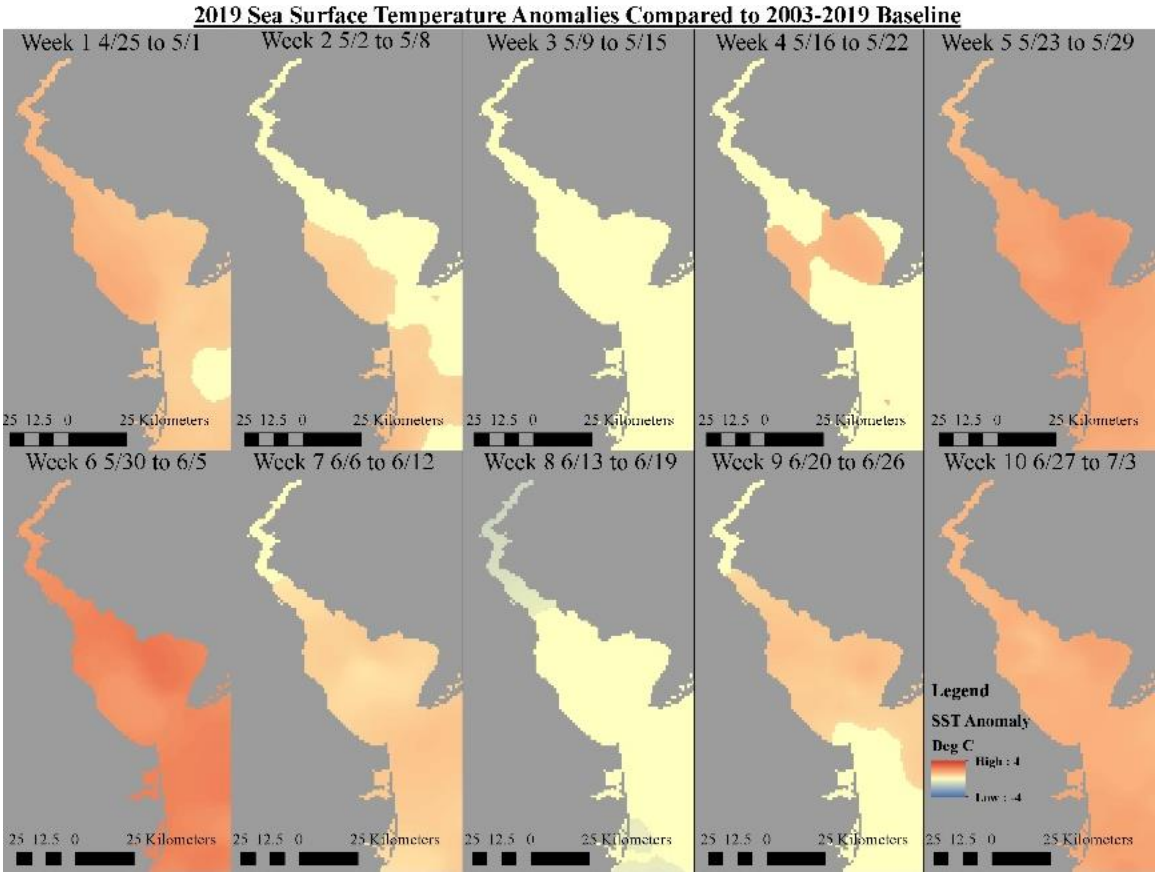

Figure 14: Weekly SST anomalies for 2019 in the Delaware Bay area compared to the baseline SST observed in Figure 7. Beige represents no statistically significant anomaly,

warmer colors as statistically significant higher SSTs, and cooler colors as statistically significant lower SSTs

The SSTs observed in 2020 do not coincide with data collected for HSC, however it is the coolest year concerning SST as seen in Figure 15. No anomalous SST was detected in Weeks 1 and 6, along with Week 2 – excluding a small geographic area in the Southern region of the Bayshore area approximately 1° C. Cooler anomalies, specifically in Weeks 3 and 4, ranged between -1° to -2° C throughout the Bayshore area. Warmer anomalies this year are present, but are restricted only to the Northern and Central regions in Weeks 7 through 10 ranging between 1° to 2° C.

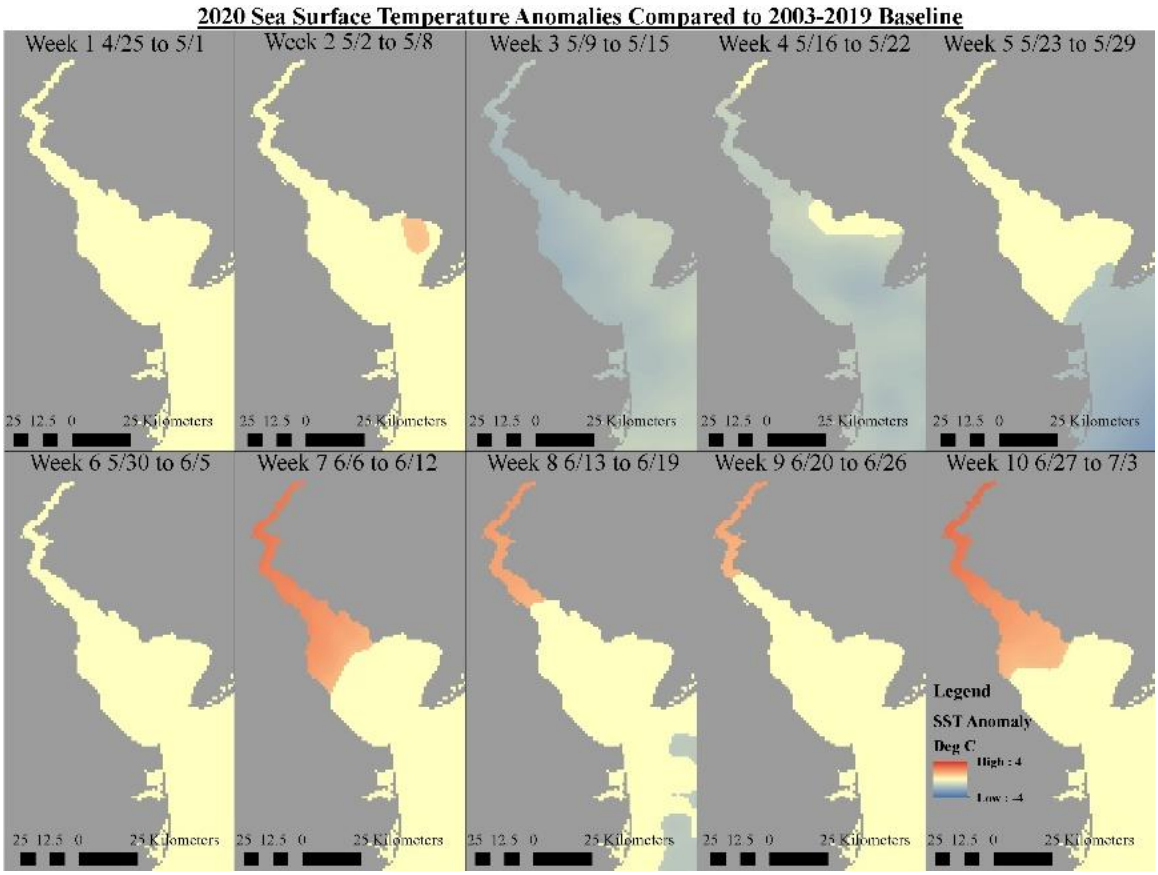

Figure 15: Weekly SST anomalies for 2020 in the Delaware Bay area compared to the baseline SST observed in Figure 7. Beige represents no statistically significant anomaly, warmer colors as statistically significant higher SSTs, and cooler colors as statistically significant lower SSTs.

Patterns in SST for Geographic Regions

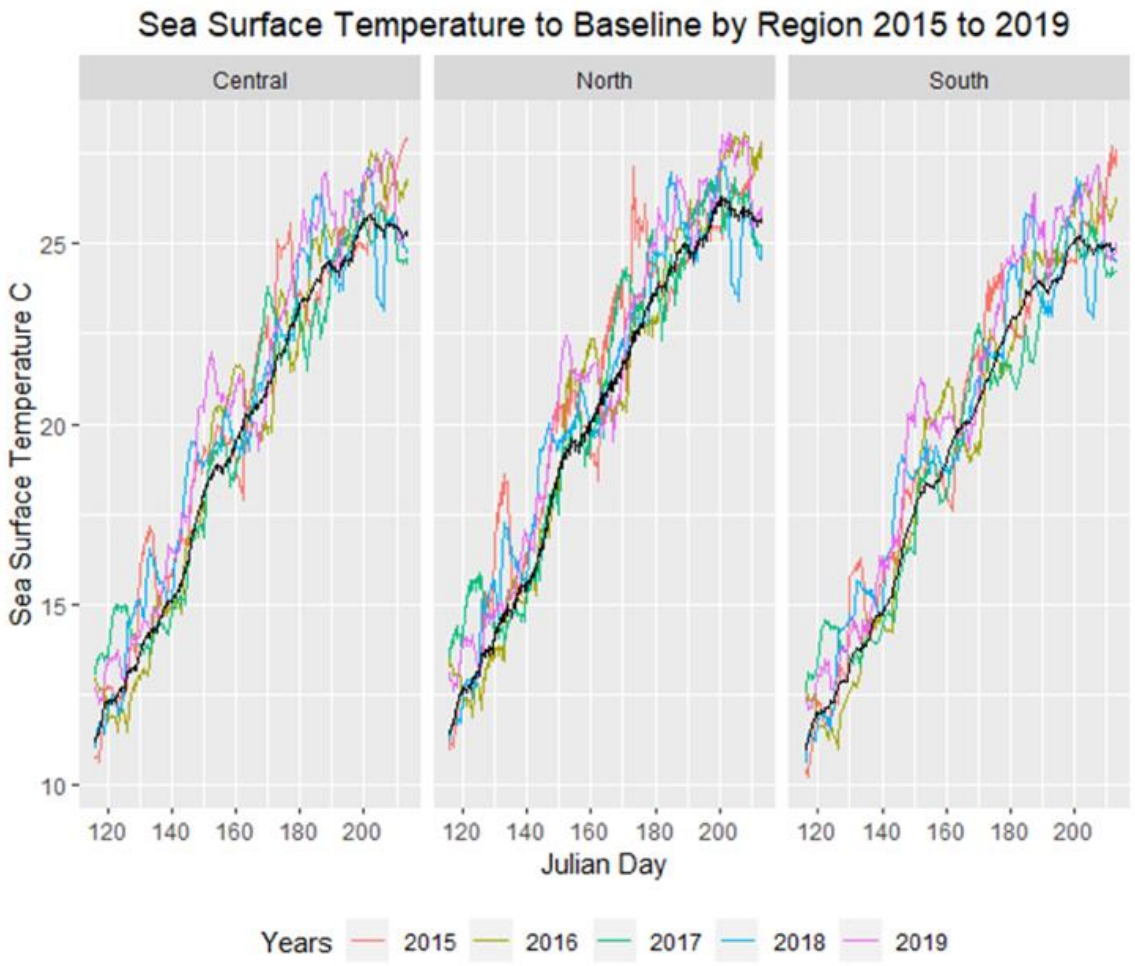

Figure 16: Change in SST from April 25 to July 31 between the years of 2015 and 2019 compared to the baseline SST.

SSTs by geographic regions, as seen in Figure 16, shows how SSTs increase during the HSC spawning season as the seasons transition from mid-spring to summer. SSTs vary between individual years but increases in the same general fashion when compared to the baseline. Although the variation between all three geographic regions, the SST are highest in the Northern region and lowest in the Southern region of the Bayshore area by approximately 0.5° to 1° C. Although the Central region is cooler than

the Northern region and warmer than the Southern region, it does exhibit a higher variation in SSTs than the other geographic areas.

Correlation Between MUR and Buoy Observations

t-Test: Paired Two Sample for Means								
	Mean C°	Variance	Observations	Hypothesis	df	t Stat	p-Value	Correlation
Towns Bank MUR	20.4	21.8	98	0	97	-2.5026	0.007	0.958
Cape May Buoy	20.0	12.1	98	0	97			

Table 6: Comparison of the in-situ and MUR dataset shows that there is a statistically significant difference between these two datasets, resulting in observations from the MUR dataset to exhibit a slightly warmer SST measurement. Despite the significant difference, they are both highly correlated.

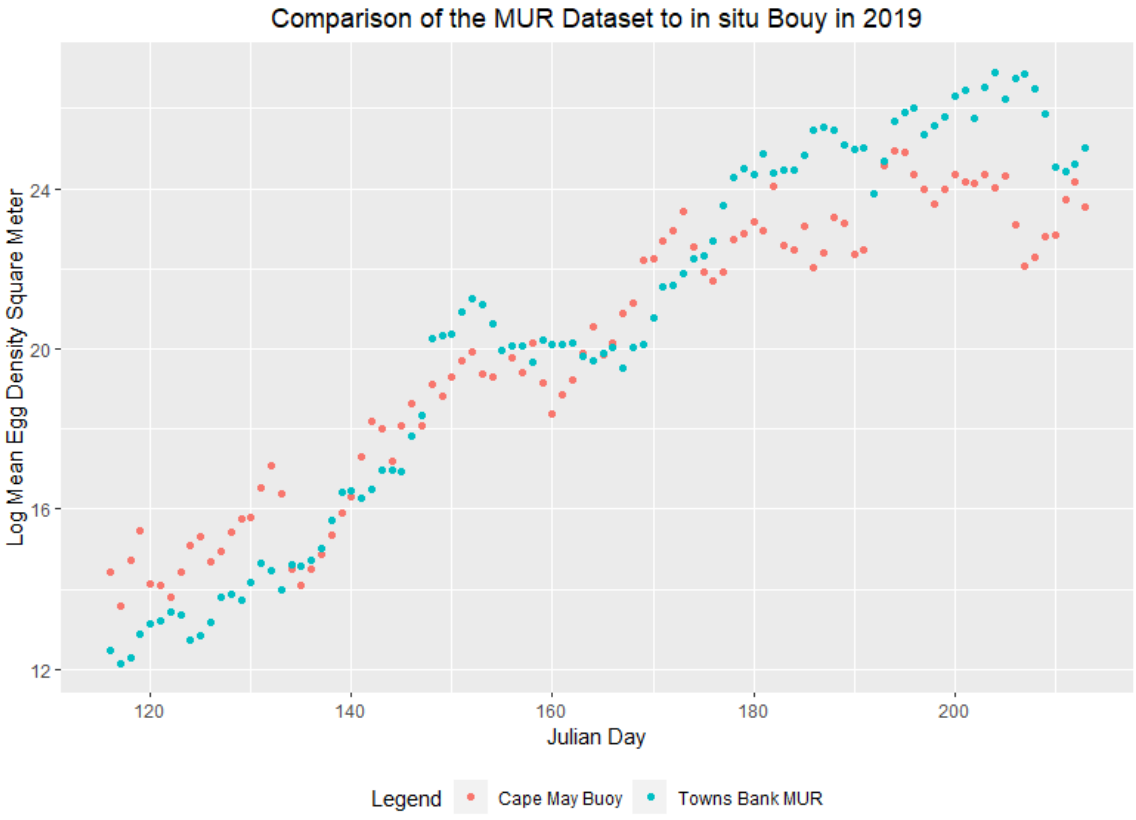

Figure 17: Comparison of the daily mean SST from the MUR dataset to the nighttime observations of an in-situ buoy located in the Delaware Bay.

Comparing the nighttime mean SST from *in-situ* buoy observations to the daily mean determined from the MUR dataset, observed in Figure 16, reveals that the two datasets are statistically different based on a two sample t-Test, as seen in Table 5. This difference shows warmer observations from the MUR of approximately 0.4° C, during the 2019 spawning season. Despite the differences between these two datasets they are highly correlated to each other, as observed in Figure 18 in Table 5.

Determining SST Threshold for Peak Spawning – Classification Tree

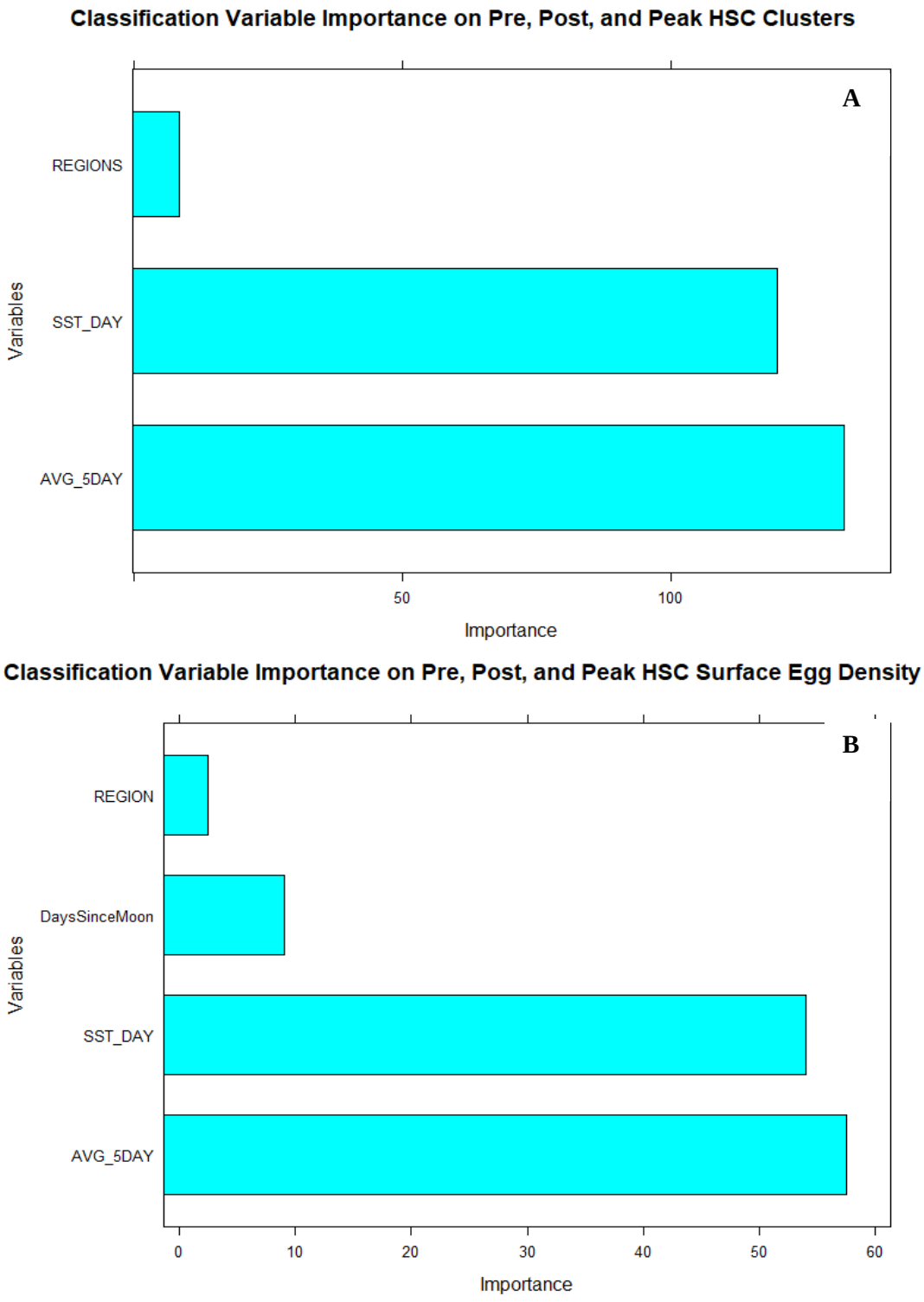

Figure 18: Variable importance for determining pre, post, and peak abundance for HSC clusters (a) and surface egg densities (b). In both classification trees the five-day moving average was the most important variable.

Classification trees were constructed to determine if a SST threshold could be determined to identify the peak abundance for mean clusters per transects and surface egg densities using variables influencing the entire Bayshore area including the SST on the day of sampling, a five-day moving average of SST, the geographical regions, and the number of days since the new or full moon. Although all the aforementioned variables were used their importance differed between the two classification trees, as seen in in Figure 19a and b. The five-day moving average was determined to be the most important classification variable, followed by the SST on the day of sampling. Region was the least important variable used in the classification, however the number of days since the new or full moon was only used in the classification tree for surface egg densities.

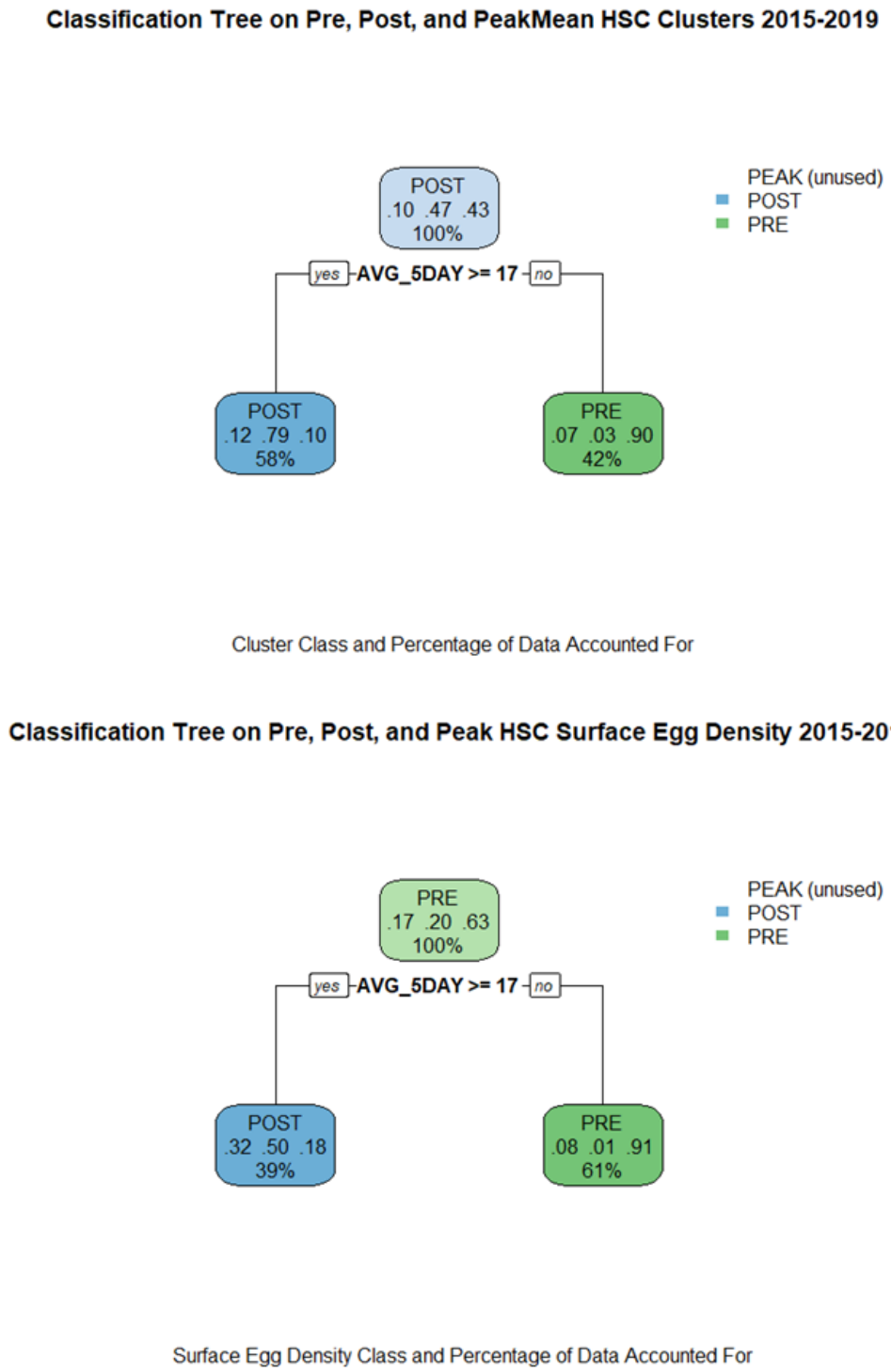

Figure 19: The pruned classification trees for identifying the peak abundance of (a) HSC egg clusters and (b) HSC surface egg densities on beaches in the Delaware Bay between 2015 and 2019. A temperature of 17° C as a five-day moving average was identified as a

threshold to determine when HSC abundance changed from pre-peak abundance to post-peak abundance.

The classification trees were pruned using the lowest cross-validation error for the cost complexity parameter (CP), creating the trees for HSC egg clusters and surface egg density as seen in Figures 20a and b. The trees with the lowest error resulted in the detection of a temperature threshold of 17° C for the five-day moving average for SST. The training data for clusters classified 42% as pre-peak and 58% as post-peak, with a model accuracy of 81.4% utilizing the testing data on the trained model. The training data for surface egg density classified 61% of the as pre-peak and 39% as post-peak, with a model accuracy of 80.4% utilizing the testing data on the trained model. In both models the peak was not used because of their limited number of observations each year compared to the other two classes, potentially contributing to the reduced accuracy in the models.

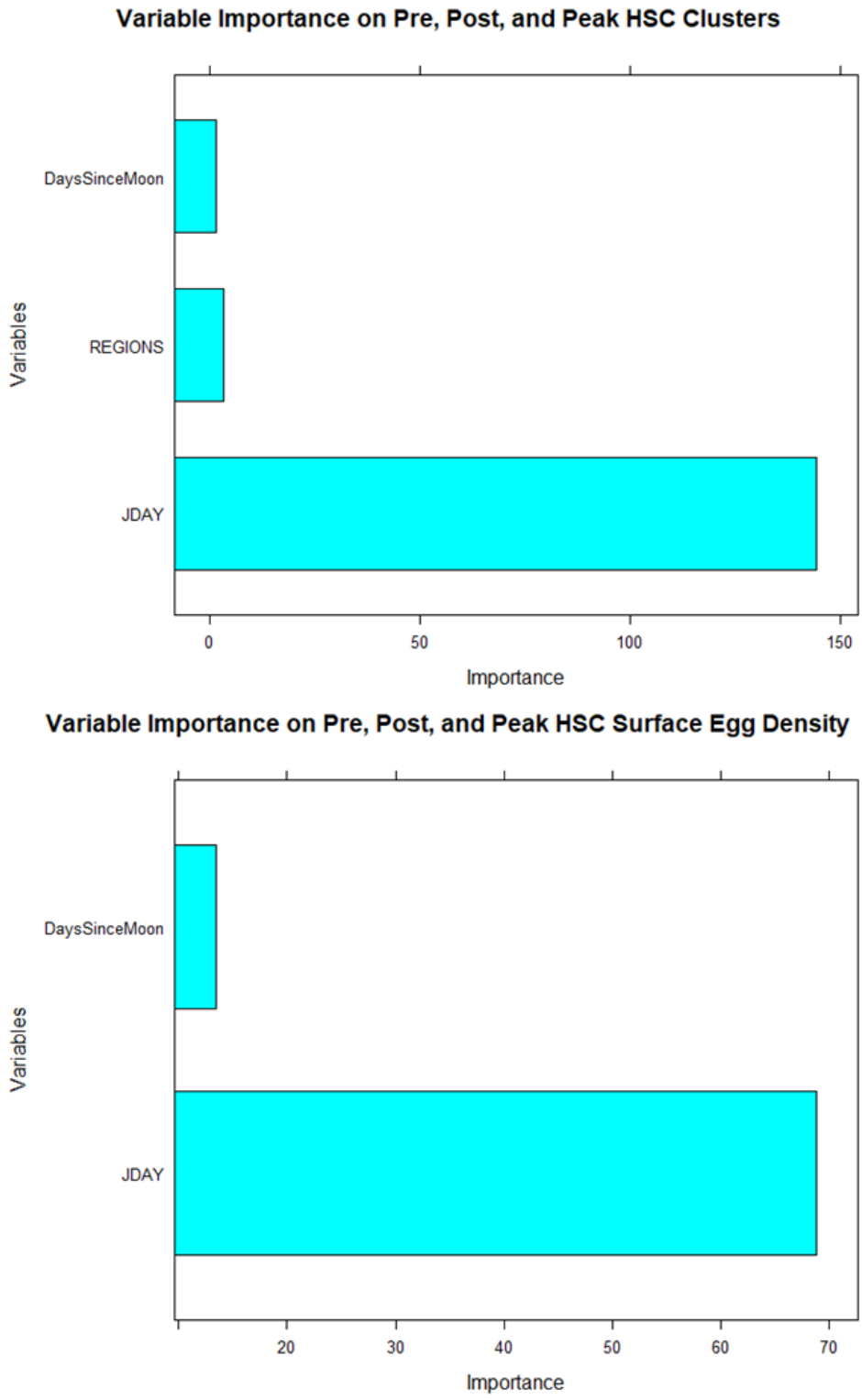

Figure 20: Variable importance for determining pre, post, and peak abundance for HSC clusters (a) and surface egg densities (b). In both classification trees the Julian Day was the most important variable.

Classification trees were also created utilizing the Julian Day to determine when peak spawning was occurring between 2015-2019, but the SST on the day of sampling and the five-day moving average were removed because of their high correlation. The variable importance identified that the Julian Day was the most important variable for both HSC egg clusters and surface egg densities – as seen in Figure 21a and b. Unlike the classification trees that utilized temperature measurements, variable importance for HSC cluster, Figure 19a, utilized both regions and the number of days since the new or full moon, while the variable importance for HSC surface egg densities, Figure 19b, only utilized the number of days since the new or full moon in its classification for peak abundance.

Classification trees to detect the Julian Day of peak abundance can be seen in Figures 22a and b, and were pruned to reduce the cross-validation error of the CP. The classification tree for clusters to predict peak abundance identified a Julian Day of 150 (May 29) as the separator of pre-peak and post-peak abundance utilizing the training data. 41% of the testing data was classified as pre-peak, while 59% of the data was classified as post-peak with an accuracy of 83.0%. Unlike the three previous classification trees to identify peak abundance, the final tree used all three classes to classify pre-peak, peak, and post-peak abundance for HSC surface egg density in Figure 20b. Days prior to Julian Day 149 (May 28) were classified as prior to the peak abundance and accounted for 64% of the testing data. Julian Day less than 157 (June 5) that was 1 or more days after the new or full moon were identified as peak abundance, accounting for 17% of the testing data. The remainder was classified as post-peak and accounted for 18% of the testing data. In full this final classification tree had an accuracy of 81.1%.

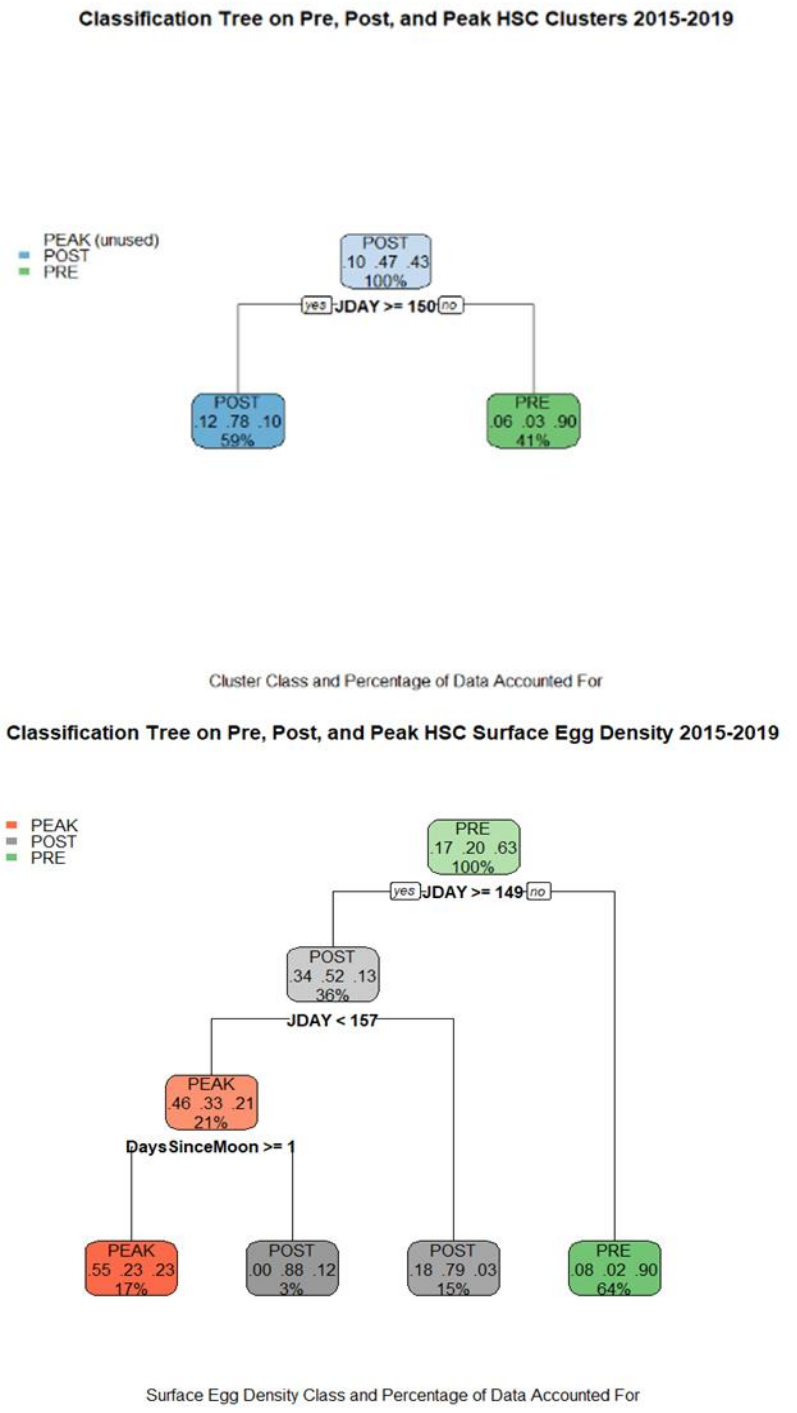

Figure 21: The pruned classification trees for identifying the peak abundance of (a) HSC egg clusters and (b) HSC surface egg densities on beaches in the Delaware Bay between 2015 and 2019. For HSC clusters (a) identified that days greater or equal to Julian Day 150 separated pre-peak and post-peak abundance. In HSC surface egg densities (b) identified that a Julian Day less than 149 was pre-peak, while post-peak was identified as greater than Julian Day 157 or less than day 157 and on the same day as a new or full moon.

Linear Regression Models of Threshold Date Change

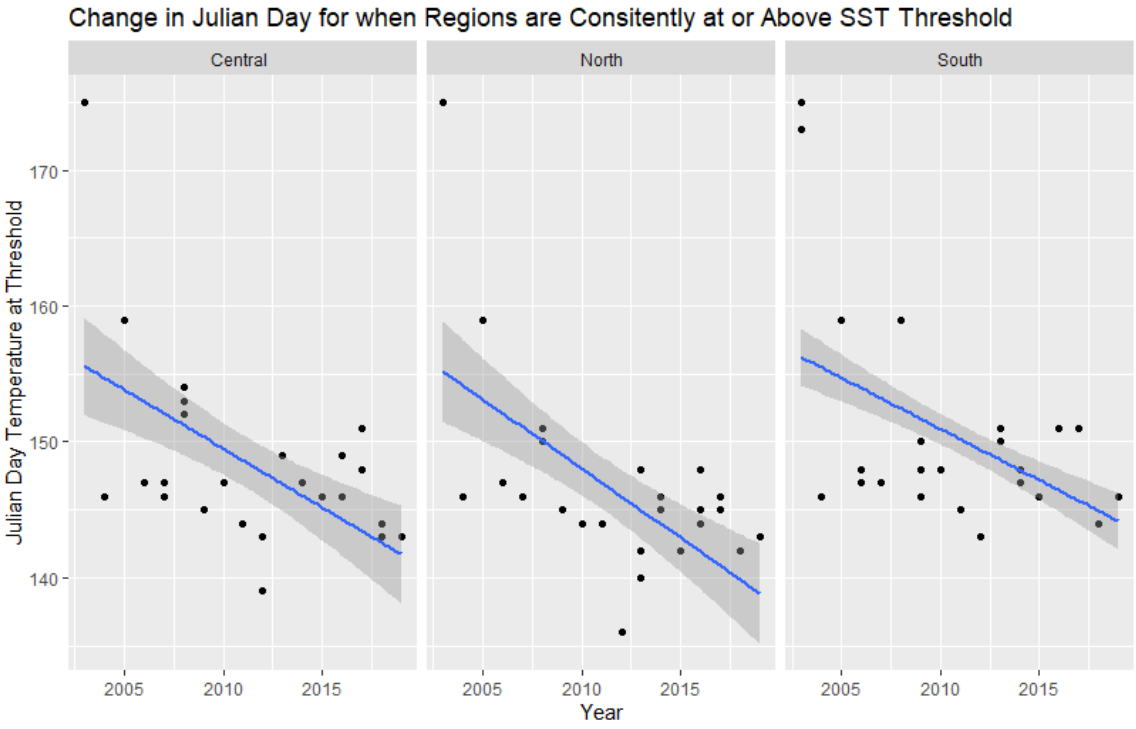

Figure 22: Linear regression models for the change in date between 2003 to 2019 when SST reaches 17° C utilizing the MUR dataset based upon the geographic regions in the Bayshore area.

Table 7: Statistics on the linear regression model observed in Figure 25 on when the geographic regions have reached the 17° C threshold, the significance of these change, and how many days it has advanced since 2003.

Regional Linear Regression Model Results							
	β	*STD Error*	*t-value*	*p-value*	*DF*	R^2	*Days Changed*
North	-1.0	0.2	-5.2	$3.7x10^{-3}$	49	0.36	-17.3
Central	-0.9	0.2	-4.6	$3.5x10^{-5}$	49	0.30	-14.7
South	-0.8	0.1	-6.7	$5.9x10^{-10}$	49	0.25	-12.8

Utilizing the 17° C SST threshold identified with the classification trees, Figures 20a and 18b, and inferred by the regression trees, Figure 24a and b, linear regression models were constructed to better understand when this temperature was reached for each geographic region and individual beaches in the Bayshore area. All three geographic regions experienced an advancement of when SSTs were consistently above 17° C, as observed in Figure 23, that was statistically significant, as noted in Table 6. The advancement showed a relationship geographically with a more rapid advancement of this threshold earlier in the year in the Northern region with a slower advancement as you move south. The Northern region has experienced an advancement of this threshold by 17.3 days, 14.7 days in the Central region, and 12.8 days in the Southern region – as

observed in Table 6.

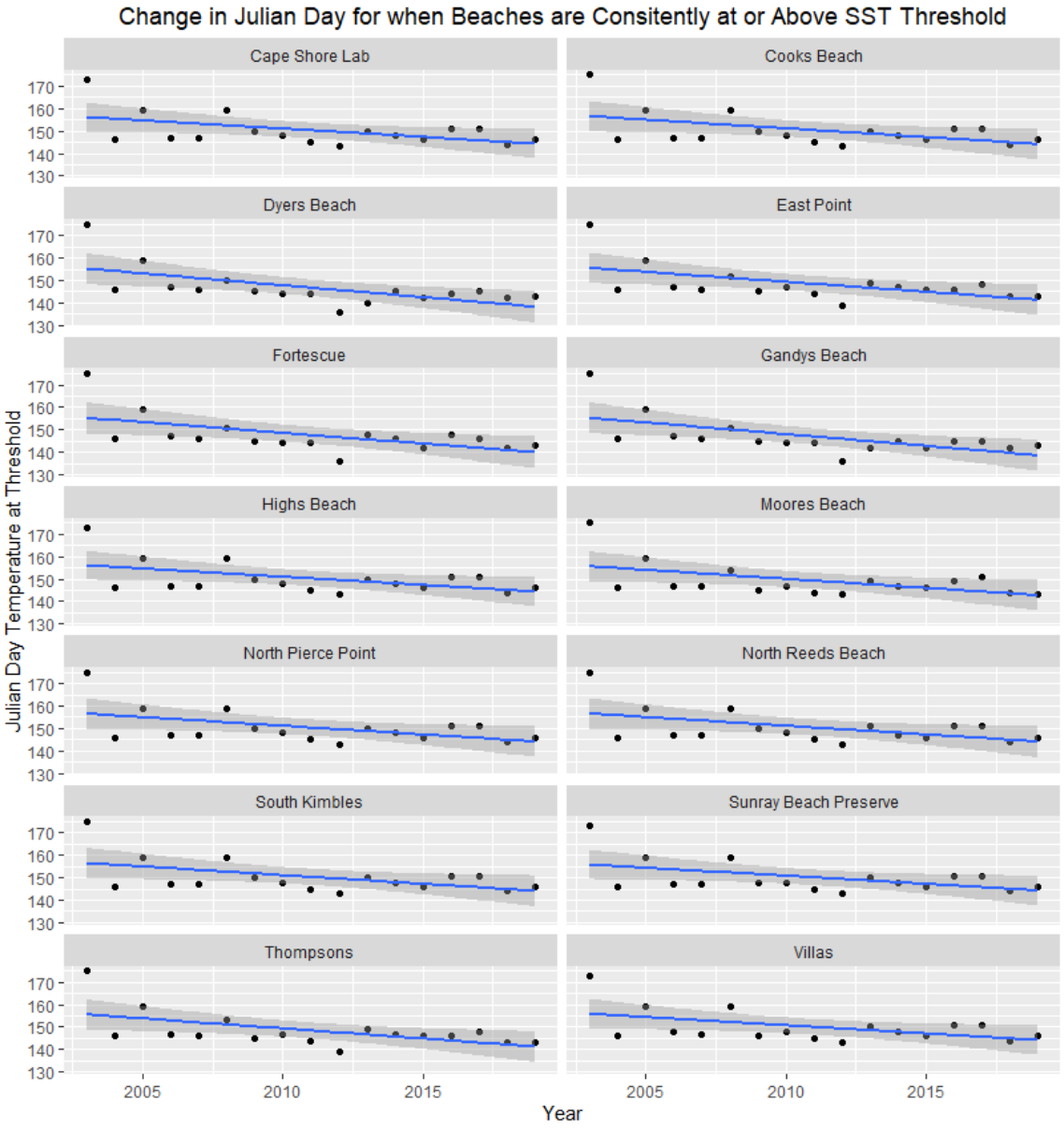

Figure 23: Linear regression models for individual beaches in the Bayshore area on when SSTs are consistently at or above the 17° C temperature threshold for HSC spawning

Table 8: Results of specific beach location linear regression models determining the advancement of when each location reached the 17° C threshold, its significance, and the number of days it has advanced since 2003.

Beach Linear Regression Model Results								
	Region	*β*	*STD Error*	*t-value*	*p-value*	*DF*	R^2	*Days Changed*
Gandy's Beach	N	-1.04	0.35	-2.99	$9.2x10^{-3}$	15	0.37	-17.7
Dyers Beach	N	-1.06	0.35	-3.02	$8.7x10^{-3}$	15	0.38	-18.0
Fortescue	N	-0.96	0.36	-2.68	0.017	15	0.32	-16.3
East Point	C	-0.89	0.34	-2.60	0.020	15	0.31	-15.1
Thompsons	C	-0.90	0.34	-2.62	0.020	15	0.31	-15.3
Moore's Beach	C	-0.81	0.34	-2.37	0.032	15	0.27	-13.7
North Reeds Beach	S	-0.78	0.35	-2.25	0.040	15	0.25	-13.2
Cooks Beach	S	-0.77	0.34	-2.25	0.040	15	0.25	-13.2
South Kimble's Beach	S	-0.77	0.34	-2.25	0.040	15	0.25	-13.2
North Pierce Point	S	-0.77	0.34	-2.25	0.040	15	0.25	-13.2
Highs Beach	S	-0.74	0.33	-2.25	0.040	15	0.25	-12.5
Cape Shore Lab	S	-0.74	0.33	-2.25	0.040	15	0.25	-12.5
Sunray Beach Preserve	S	-0.73	0.33	-2.20	0.044	15	0.24	-12.3
Villas Beach	S	-0.73	0.33	-2.20	0.044	15	0.24	-12.8

The advancement of the date for when SSTs were consistently at or above the 17° C was also observed in all beaches that had HSC egg clusters and surface egg densities analyzed, as seen in Figure 24. The advancement of this date was not the same in all beaches, however a strong relationship was observed geographically, as seen in Table 7. In the Northern region this date advanced between 16.3 to 18 days, the highest rate of advancement of all regions. The Central region exhibited advancement of this date by 13.7 to 15.3 days, while the Southern region was observed to have advanced 12.3 to 13.2 days. This close geographic relationship was further demonstrated in their R^2 and p-values which decreased from north to south.

Estimating Egg Cluster and Surface Density – Regression Tree

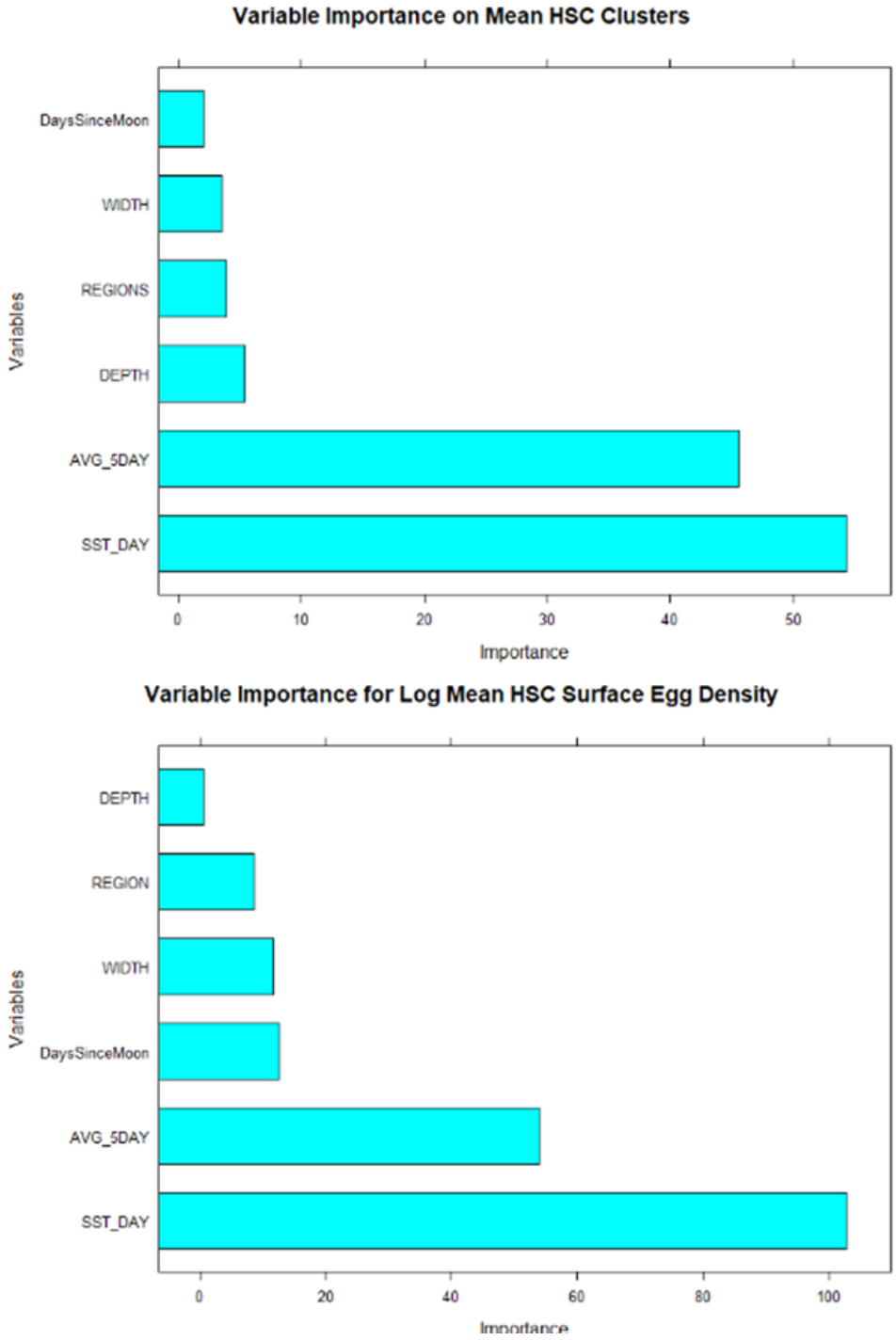

Figure 24: Variable importance for regression trees to identify the abundance of HSC clusters (a) and surface egg densities (b). SST and the five-day moving average for SST were the most important variables in the tree construction, with other variables to a lesser degree.

The regression trees were also created for both HSC egg clusters and surface egg densities to predict higher abundances in the Delaware Bay, along with the utilizing variables that are site specific including boolean values for sand depth greater than 40 cm, beach width in m, and geographic region. In both created trees the most important variables used to identify high abundance were the SST on the day of sapling and the five-day moving average for SST, as seen in Figures 25a and b. These two variables are closely related, however individual regression trees were not created to separate these variables because they did not significantly change the final trees constructed. Unlike the classification trees, all the variables used showed some degree of importance in the construction of the regression tress. Variable importance did differ between HSC egg cluster and surface egg densities with depth and geographic region being more important for clusters observed in Figure 25a, while the number of days since the new or full moon and beach width being more important for surface egg densities as seen in Figure 25b.

The regression trees were pruned using the lowest cross-validation error for the CP, creating the final trees for HSC egg clusters and surface egg density as seen in Figures 26a and b. The lowest predicted HSC egg clusters per transect, Figure 26a, occurred when the SST were less than 15° C or a five-day SST moving average and SST were greater than 21° C with predicted mean clusters of 0.23 and 0.29 per transect respectively accounting for 44% of the testing data. The highest predicted mean clusters per transect emerged when SSTs exceeded 16° C with a larger beach width exceeding 22 m and a sand depth greater than 40 cm. These criteria predicted that the mean clusters per transect would be approximately 1.4 and accounted for 5% of the testing data. The RMSE of the model was determined by utilizing the testing data and was calculated to be 0.49.

The lowest predicted HSC surface egg densities, Figure 26b, emerged with SST values lower than 15° C with a log average of 2.2 m^2 accounting for 24% of the training data. Higher densities were observed with higher SST with a 3.8 log average m^2 when SST exceeded 18° C or a minimum of 2.4 log average m^2 when SST was just above 15° C. Geographic region also played a role in this regression tree with higher densities observed in the Central or Southern Regions compared to the Northern region whe SSTs were between 16° and 18° C. Finally, lunar cycles also influenced surface egg densities with higher abundance observed closer to the new or full moon. The RMSE was determined to be 4.1 when utilizing the testing data.

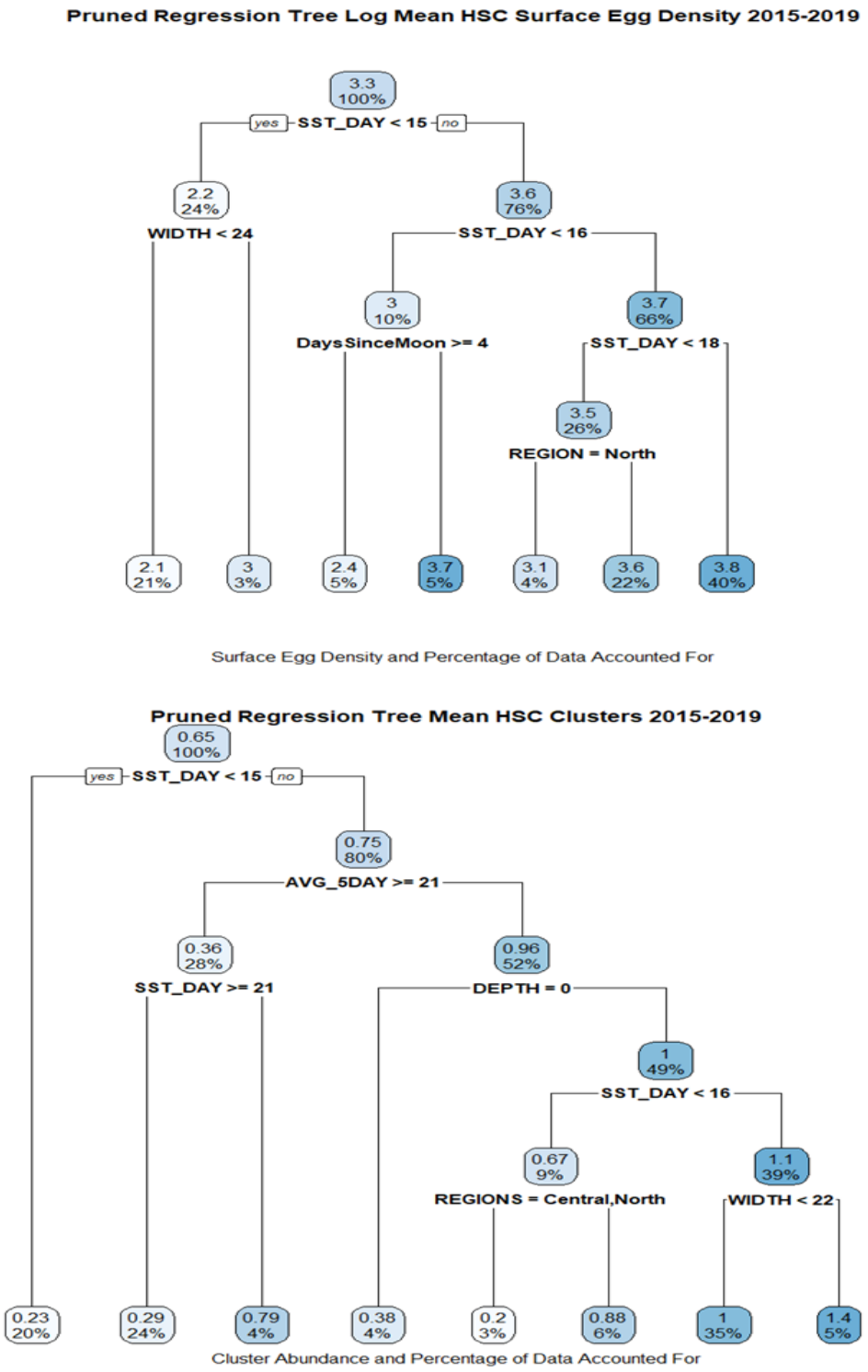

Figure 25: Regression trees for HSC clusters (a) and surface egg densities (b) using SSTs and local variables from individual beaches. Both trees identify that the lowest abundances emerge with a SST less than 15° C and highlight geographical patterns with lower abundances in the Central and Northern regions in HSC clusters and in the Northern region in the surface egg densities.

Discussion

SST in the Bayshore Area for Regions and Beaches

The MUR dataset in 2019 for Town Bank compared to the *in situ* Cape May buoy was observed to be statistically different, although they were highly correlated as seen in Table 5 and Figure 18. The MUR dataset was observed to have a mean difference that was approximately +0.4° C compared to the buoy, suggesting that the MUR dataset has a slight warming bias than *in situ* measurements. This consistent bias is most likely attributed to the blended analysis to synthesize the MUR dataset that incorporates satellite measurements that may only read the skin SST compared to the foundation SST that traditional buoys measurements record (Okuro, et al., 2014). The differences between these two datasets are also comparable with more detailed work conducted by Chin *et al.* (2017) that suggest that the MUR dataset agrees with the foundation SST averaging 0.36º C. Despite the slightly warmer values between these two datasets MUR provides detailed information on SST in the near-shore area that has a spatial resolution an order of magnitude greater than other SST products currently in existence (Chin, et al., 2017), allowing detailed information to be extracted over greater geographic areas with low or limited *in situ* observations.

As expected, SSTs in the Delaware Bay increased from mid-spring on April 25 (Julian Day 116) to mid-summer on July 31 (Julian Day 213). Most temperatures in the area – as seen in Figure 9 – are approximately 10° C at the end of April and can exceed 25° C by the end of July – particularly in the Northern region. SSTs in the Delaware Bay begin to increase rapidly from approximately 12.5° C on Week 2 to 20° C by the end of Week 7 as the days grow longer and warmer, then begins to plateau by Week 10 towards

the end of July as SST becomes more homogenous during the warmest month of the year (Weather, 2020). Although the entire Bayshore area is warming during this time period, warming is not uniform in the area. The Northern region warms the fastest compared to the Central and Southern regions as it is shallower and receives warm surface water from the Delaware River that may contribute to its early warming pattern. The cooler SSTs in the Southern region are most likely attributed to its proximity to the ocean, a much larger and deeper volume of water that requires more time to warm and homogenize with the other two regions.

These geographic warming patterns are clearly visible when observing the regional SST baselines in Figure 16, although the three baselines show a similar warming pattern, the Northern region is 0.5° C and 1.5° C higher than the Central and Southern regions. Similar warming patterns also emerge when looking at the regional temperatures for individual years in the same figure. Although variation in temperatures exhibits more significant variation for individual years when compared to the smoothed baseline compring daily observations over a 17 year period, warmer temperatures than the baseline appear to dominate than colder temperatures – especially in the Northern region. These patterns also emerged for the individual beaches that comprise these regions as seen in Figure 17, however not all of the variation observed was statistically different from the baseline temperatures.

In the Northern region only cooler anomalies for SST were observed in Week 3 and 4 in 2020 along with Week 2 in 2016, while the remaining observations were normal or significantly warmer than expected between 2015 to 2020 – as seen in Figures 10 to 15. The more frequent warmer anomalies could be caused by 3 specific interacting

factors: (1) input of warm less dense freshwater, (2) limited tidal mixing between warm freshwater and ocean water, and (3) shallower waters in this region that warm more quickly. The water that empties from the Delaware River in this region may be warming more quickly do to assistance from the land surface from higher atmospheric temperatures, resulting in more rapid warming as the freshwater is less dense than saline water potentially being detected more frequently in the remotely sensed data that is used in the MUR dataset. This influence is most likely diminished further south due to increased tidal mixing in the Central and Southern regions limiting warming of SST from freshwater and increasing the depth further south.

The Central and Southern regions display more variation in the appearance of anomalous SST with both regions displaying warmer and cooler anomalies. Cooler anomalous SSTs were apparent in Weeks 2 through 5 in 2016 and 2020, however warmer or typical temperatures predominated in the remaining weeks between 2015 and 2020. 2018 and 2019 stand out as warm years, especially during the early spawning periods of HSC between Weeks 1 through 6. In this work it is believed that increasing SSTs during the spawning season was the main driver that initiated high spawning periods resulting in peak egg cluster and surface densities in the Bayshore area, while moon phases were the secondary driver if suitable temperatures existed to increase the abundance of egg clusters and surface densities. As these dynamics influence the timing of HSC spawning it can create changes in the spatial distribution of HSC eggs in the Bayshore area and when periods of high abundance emerge, deleteriously impacting migratory shorebird populations that rely on this energetic resource (Smith, et al., 2011; McGowan, et al., 2011; Tucker, et al., 2019).

Despite the patterns that have been previously discussed, it is important to consider that this analysis has potentially undercounted warmer SST anomalies in the Delaware Bay during the spawning seasons between 2015 to 2020. Baseline SSTs were composed of data between 2003 to 2019 which is shorter than a traditional 30 year baseline due to the limited timeframe of the MUR dataset. During the 17 year period used to create the baseline 9 of the 10 warmest years on record have emerged since 2005, which may have assisted in increasing SST observations. Because of this potential bias it is important to consider that warmer anomalies may have been undercounted with cooler SSTs being overcounted in either the severity of the determined anomaly or masked entirely. Despite the potential warming bias in the MUR dataset in the creation of the weekly SST baselines, it is likely that the detected warm anomalies may be more severe than were determined if a longer baseline was able to be created in this analysis.

Regional HSC Egg Clusters and Surface Densities

Regionally HSC egg clusters and surface densities were observed to increase gradually early in the spawning season between 2015 to 2019 prior to Julian day 130 (May 9), and quickly accelerated towards their periods of peak abundance observed in Tables 3 and 4 for the given years. Unlike the sampling that occurred for egg clusters the sampling for surface density ended early in the first week of June. This occurred because the sampling of surface egg densities was designed to better understand the abundance of eggs on the surface of Bayshore beaches when the red knots are historically present – traditionally arriving between Julian day 141 (May 20) and exiting 158 (June 6) (Tispoura & Burger, 1999). After this date high egg densities that are present may be

available for other avian species in the area such as the Ruddy Turnstone (*Arenaria interpres*) or Semipalmated Sandpiper (*Calidris pusilla*), however the resource would not be present for the red knots (Tispoura & Burger, 1999; McGowan, et al., 2011). Although this suggests that sampling may not have completely captured the entire spatial distribution of HSC eggs on the beach surfaces, patterns do still emerge geographically concerning this key resource abundance.

The rapid increase in HSC egg clusters between the years of interest observed after Julian day 130 (May 9) corresponds to the Week 3 baseline when SSTs typically range from 13.5° to 15.0° C. These findings corroborate previous observations that more HSC begin entering the Delaware Bay and increase in activity when SSTs in May reach 13.7° to 16.3° C (Smith & Michels, 2006; Smith, et al., 2010). As more HSCs begin entering the Bayshore area and make their way onto the beaches to spawn as SSTs become more suitable, the average number of clusters per transect and surface egg densities increases rapidly towards their peak abundance between Julian day 149 and 160 (May 28 to June 8) observed in Tables 3 and 4. The timing of the peak spawning events within the Delaware Bay during these years typically fell within 7 to 10 days of each other between regions, suggesting that spawning individuals are responding to the same environmental signals to initiate spawning – despite higher SSTs in the Northern region. After this peak period abundances for clusters were observed to plateau and then decrease, however this was not observed in the surface egg densities due to the early cessation of sampling. Although the complete distribution on surface egg densities were not captured the do its early ending they did begin to plateau, suggesting that they were

either approaching peak or at their peak densities for the given years – with the exception of 2019 that had limited sampling completed.

Mean HSC egg clusters and surface densities for all three regions showed variability in abundance between years, however they did show increasing trends between 2015 to 2019 – with the exception of the Central region for clusters. The increasing trends were more pronounced for the Northern region than the other two, potentially caused by warmer SST providing refuge for spawning HSC during cooler years such as 2016, increasing salinity over time as sea-levels rise, more preferable characteristics found on these specific beaches, or other factors not considered here. Despite the observed positive trends for both HSC egg clusters and surface egg densities, none of them were significant and supports the current belief that the spawning population in the Delaware Bay are either stable or increasing but requires more observations to make definitive conclusions regarding HSC population changes (Smith, et al., 2017).

Individual Beach HSC Egg Clusters and Surface Densities

Although patterns concerning the HSC egg clusters and surface densities emerged geographically by region, not all sites within the same region or year showed similar abundances. In the Northern region Gandy's Beach consistently had the lowest cluster abundances as the most northern location in the region and amongst the studied beaches as a whole. Despite the lowest cluster abundances when compared to Dyer's Cove and Fortescue, it frequently did have higher than anticipated surface egg densities in the region – with the exception of 2018 and 2019 – compared to the low number of clusters.

This may be caused by the incoming tide as eggs are mobilized northward as the tide enters the Bayshore area and are deposited as it retreats. Fortescue consistently had the highest cluster abundances in the region and the highest surface egg densities in 2018 and 2019. This is most likely due to sand depths that frequently can surpass 40 cm and with an average width of 18.2 m, suggesting that Fortescue has more favorable beach characteristics in the region when compared to Dyers Cove and Gandy's Beach.

The Central region had the lowest cluster abundances between the three regions, but East Point specifically stands out as having the lowest abundances at any given year and region. Despite the low cluster abundances it does have comparable surfaces densities between 2015 and 2017 with other locations in the Central region suggesting that localized currents or tidal cycles may be mobilizing eggs from other locations in the Bayshore – within or beyond the Central region – creating higher surface densities than processes such as bioturbation and wave action could account for when looking solely at its singular location. This may also be the case for Moore's Beach which also hosts low cluster abundances when compared to Thompsons, but also has similar surface egg densities. The higher cluster abundances on Thompsons Beach also coincide with an average sand depth of 21.8 cm and a beach width of 20.7 m, suggesting that this location may have more favorable beach conditions compared to East Point and Moore's Beach.

The Southern region has the highest cluster abundances and surface egg densities between the three regions, with the lowest abundances observed in the more southern regions of the area such as in Villas or Cape Shore Lab. Sand depths for Cape Shore Lab were the lowest in this region with an average depth of 18.0 cm and a beach width of 12.5 m suggesting that it may not be considered suitable habitat when compared to other

beaches in the region that are both wider and have greater sand depth for clusters. The beach at Villas does have sufficiently high sand depths averaging 38.6 cm and a beach width of 18.0 m, however its proximity to the ocean may have increased wave heights or have reduced SSTs to have HSC select a different more favorable location in the region to spawn.

Cooks Beach, North Reeds Beach, and Highs Beach have the highest observed egg clusters and surface densities in the Southern region. These three locations have average sand depths of 24.7 cm, greater than 40 cm, and 29.3 cm respectively, however sand depths in all three of these locations were frequently observed to be greater than 40 cm recorded as boolean values and lower average sand depth could be caused by the location depths were measured along the transect. Along with having suitable sand depths, the widths of these beaches were generally wider than other locations with 20.7 m at Cooks Beach and 23.7 m at North Reeds Beach. The exception in this case is Highs Beach with a relatively thin width of 14.5 m. These locations were previously observed by Jackson *et al.* (2020) that wave heights beyond storm events do not typically exhume large numbers of clusters, potentially accounting for the large cluster abundances. Likewise it was also observed in these locations that bioturbation plays a significant role in bringing eggs to the surface, particularly during peak spawning days (Jackson, et al., 2020). This could make these locations a significant source of eggs to become transported to other locations in the Bayshore area and account for the high densities on the beach surface in locations that had higher than expected surface densities.

Classification Trees for Peak Abundance

The classification trees to identify the conditions for peak abundance for HSC egg clusters and surface densities emphasized the importance of the correlated values for SST and Juilian day, but also the five-day moving average for SST. Although the five-day moving average is also correlated with the SST and Julian day, it provided a better long-term understanding of SSTs in the Bayshore area that HSCs may be responding to and was consistently identified as a more important variable than the SST for the specific day spawning occurred – as seen in Figures 19a and 19b. The geographic region was considered in both classification trees to be minimally important, suggesting that spawning in the region may be initiated by a signal environmental cue impacting the entire Bayshore area. Although it is widely believed this signal is the proximity to the new or full moon that influences tidal pressure (Smith, et al., 2002; Chabot & Watson, 2010; Smith, et al., 2010; Smith, et al., 2017), this was found only to be important for classifying peak surface density not egg clusters. This observation suggests that enhanced tidal cycles may increase the number of eggs mobilized during the new or full moon from HSC burrows as the tide can allow waves to more directly influence Bayshore beaches bringing more eggs to the surface and increasing densities.

When temperatures are excluded from the classification tree and replaced with the Julian day, the day is the most important variable in the construction of the trees – as seen in Figures 21a and 21b. Regions were minimally important to classifying HSC clusters, similarly to the importance that utilized temperature data, however in this case the number of days since the new or full moon was utilized to partition the data but was not a highly significant variable. The number of days since the new or full moon was also used

to construct both classification trees for extracting when periods of abundance emerged, however regions were not utilized for surface density. Because of the minimal influence regions played on these classifications and the limited importance of the number of days, it is likely that that temperature is the predominant driving force that initiates spawning in the entirety of the Bayshore area.

Classification Trees – Date and Temperature Threshold Determination

The classification trees for when the current peak abundances are occuring were identified as Julian day 150 (May 29) for HSC egg clusters and between Julian 149 to 156 (May 28 to June 4) for surface egg densities – as seen in Figures 22a and 22b. These observations suggest that egg clusters peak before surface density in the Bayshore area, with surface densities reaching their peak following the new or full moon. As spawning HSC arrive on the beaches in the Delaware Bay and dig nests to lay their egg clusters, they disturb clusters previously laid by other HSCs and mobilize their eggs through continued bioturbation and wave action bringing them to the surface. This currently agrees with previous observations in the Bayshore area that suggest HSC begin spawning in mid-May and peak towards the end of the month and into the beginning of June when the red knots are in the area before they leave to finish their spring migration (Tispoura & Burger, 1999; Smith & Michels, 2006; Smith, et al., 2010; Smith, et al., 2017).

The classification trees that utilized temperature for both HSC egg clusters and surface densities in the Bayshore area identified that when the five-day moving average for SST reached 17° C there was a shift from pre-peak to post-peak abundance as seen in Figures 20a and 20b. The identification of the same temperature in both classification

trees and the minimal importance of region and days since the new or full moon, suggests that temperature is the driving force for spawning behavior (Smith, et al., 2002; Smith, et al., 2010; Shuster, 2015; Smith, et al., 2017). Despite the influence of temperature other factors are capable of delaying spawning even if temperatures are suitable such as storm events or periods with high wave activity.

To investigate this interaction between how higher temperatures can influence when spawning can occur the years 2017 and 2018 are helpful examples of this dynamic. As seen in Figure 12 2017 represented typically SSTs during the peak of the spawning season identified in the classification trees, or more specifically Weeks 5 and 6. SSTs prior to this were typical during Weeks 3 and 4, resulting in peak clusters to occur on Julian day 160 (June 8) in the Northern, 165 (June 13) in the Central, and 156 (June 4) Southern regions. Spawning this year was slightly later than expected, most likely caused by the stormy conditions that dominated the region from Julian day 146 to 151 – May 25 to May 30 (Robinson, 2017). Despite weather that may have existed to delay the spawning, peak surface egg densities were observed on Julian day 151 (May 31) in the Northern, 150 (May 30) in the Central, and 155 (June 3) in the Southern region – potential caused by the abrupt end in surface egg sampling around this time.

2018 did experience slightly cooler SSTs than 2017 during Week 1, however warmer SSTs predominated in May between Weeks 2 and 5 as seen in Figure 13. May was also considered to be the 5th warmest May on record exceeded only by 2015, 2004, 1991, and 2012, with air temperatures exceeding 29.4° C near Cape May on May 20th (Robinson, 2018). In response to the warmer SSTs HSCs spawned earlier and reached their peak abundance on Julian day 141 (May 20) in the Northern, 170 (June 19) in the

Central, and 151 (May 31) in the Southern regions. Despite the discrepancy in the Central region, peak surface densities also advanced compared to the previous year 143 (May 22) in the Northern, 149 (May 29) in the Central, and 151 (May 31) in the Southern regions.

Comparing these to years shows that peak clusters advanced in the Northern and Southern regions by 19 and 4 days respectively. Advancement for peak surface densities also occurred by 8 days in the Northern, 1 day in the Central, and 4 days in the Southern regions. SSTs were the warmest in the Northern region by 1.5° to 2.5° C during a majority of Weeks 2 to 5, displaying similar advancement proposed by Smith and Michael's (2006) that suggests HSC advance their spawning by 4 days for every 1° C, which is also similar to the patterns observed for surface densities in the Central and Southern regions which were also warmer but not as extreme as the Northern region. The large advancement in the Northern region was most likely caused by warmer temperatures that caused HSC to spawn earlier, however they may have been to warm to spawn similarly to the other regions since it is believed that the 17° C threshold for HSCs to spawn at this temperature is because of an evolutionary adaptation for egg incubation in beach sediments (Smith, et al., 2017). As climate change continues to increase ocean temperatures, it is important to further understand how HSCs may respond if this temperature threshold is advancing earlier in the season.

Threshold Advancement – Regions and Beaches

As previously shown with the HSC egg cluster and surface density data between 2017 and 2018, HSCs can begin spawning earlier in the season in response to warmer SSTs. Likewise spawning can also be delayed due to storm events, however in both scenarios they can deleteriously impact the availability of food for migratory birds that

utilize this key stopover location. Although storms can delay spawning by several days as in 2017, higher SSTs can advance spawning by over a week – as seen in the Northern region in 2018. This advancement also existed in 2012 when SSTs were observed to have been over 3° C warmer in the Delaware Bay resulting in the peak spawning period to occur in Julian day 143 (May 22) and in the Great Bay, MA, spawning occurred two weeks earlier due to exceptionally warm ocean temperatures (Swan, et al., 2012; Watson III, et al., 2016). With the identification of the 17° C threshold from the classification trees, linear models for when this threshold was reached for all regions and beaches can be determined to better understand potential spawning behavioral changes in the Bayshore area.

Regional patterns of when SST are consistently at or higher than 17° C between 2003 and 2019 emerge geographically with the largest advancement of this date observed in the Northern region at 17.3 days and the lowest advancement in the Southern region at 12.8 days– as seen in Figure 23 and Table 6. All regions were determined to have undergone significant advancement in when SSTs reach this threshold, suggesting that a warming climate is assisting in warming the Delaware Bay earlier than in the not so distant past. Although this advancement in when the SST threshold is met is occuring, there is variation between years in which some years are colder or warmer than expected. The coldest year was observed in 2003 resulting in the threshold not being met until Julian day 175 (June 23). Another anomalous year on the other end of the spectrum emerged in 2012 with SSTs approximately 3° C warmer resulted in this threshold advancing in all regions to Julian day 136 (May 15) in the Northern, 138 (May 17) in the Central, and 143 (May 19) in the Southern regions. When compared to typical Julian day

for spawning it had the potential to advance 12 days if we consider how spawning advances with temperature proposed by Smith and Michael's (2006), and resulted in the peak spawning period for the entirety of the Bayshore area to be observed on Julian day 143 (May 22) according to the 2012 spawning survey (Swan, et al., 2012). Although specific conclusions cannot be made that are comparable between the spawning survey conducted in 2012 to those undertaken between 2015 and 2019 due to differences in methodology, an advancement of 12 days is possible as peak HSC surface egg density emerges between Julian days 149 to 157 (May 28 to June 5) and if storm events that could delay spawning did not occur.

This same trend in the advancement of the 17° C threshold was also observed on individual beaches in the Bayshore area, but does show some variability for beaches in the same geographic region as seen in Figure 24 and Table 7. The beaches in the Northern region all show the most significant advancement of this threshold, but Fortescue advanced (15.1 days) slightly less than Gandys Beach (17.7 days) and Dyers Cove (18.0 days). However, it lagged behind by only one day suggesting that this location may require slightly more time to warm – potentially due to increased water depth or other localized factors. Thompson's (15.3 days) and East Point (15.1 days) both show similar threshold advancements in the Central region, while the advancement of this threshold at Moore's Beach (13.7 days) was more similar to advancement in the upper portions of the Southern region. The Southern region has the lowest threshold advancement, however this region could be subdivided into two different groups because of the similarity between the four northern beaches in the region and the four remaining beaches in the south. This first subgroup all experienced the same advancement (13.2

days), while the remaining beaches in the second subgroup experienced slight variation but were similar to each other (12.3 to 12.8 days). The similarities within these two subgroups is most likely due their proximity to each other. These locations are physically close to each other and utilized many of the same pixels that overlapped within the 3 km buffers that determined mean SSTs – particularly the subgroup from North Reeds Beach to North Pierce Point. The remaining beaches from Highs Beach to Villas are all close but do have more distance between them, potentially utilizing fewer overlapping pixels contributing to the slight variation.

Although each region and beach experienced significant advancement in when this threshold was met, other factors do matter that contribute to the abundance of HSC egg clusters and surface densities that are independent of storm events and weather that may alter when they spawn and assist in determining which beaches are desirable for spawning. HSCs do not display a fidelity for specific beaches in the Bayshore area and as physical conditions change HSCs may select different beaches for spawning between years (Bottom, et al., 1988; Smith & Michels, 2006; Smith, et al., 2017). As the timing of this spawning may begin to shift earlier in the year understanding the physical parameters that assist with increasing the expected abundance of HSC egg clusters and surface densities will assist in policy initiatives related to HSC conservation to assist in their population rebound and increase the abundance of this energetic resource over time to encourage the population rebound of species such as the red knot.

Regression Trees for Abundance

Regression trees are a useful method to make predictions on continuous datasets that can utilize numerical and categorical data to determine how independent variable interactions influence the dependent variable in ecological datasets (De' ath & Fabricius, 2000). Regression trees to predict abundance of HSC egg clusters and surface density at individual beaches showed that SST and the five-day moving average for SST were observed to be important to identify abundance, but other factors that influence specific sites do emerge. Beach width, sand depth, days since the new of full moon, and region were all observed to be important to identify average cluster abundance, while these same factors – with the exception of sand depth – were also identified as important variables for the identification of surface densities as seen in Figures 25a and 25b. Sand depth greater than 40 cm is likely considered to be important for clusters as they are laid at depth in burrows and shallower sand depths may encounter mud or peat that may contain compounds such as hydrogen sulfide, that are identified by HSCs as being less suitable for spawning (Bottom, et al., 1988). This is not the case for surface densities as they are brought onto the surface through bioturbation or wave action that transports them between beaches and regions – independent sand depth – that increases densities in the tidal zone (Jackson, et al., 2020). This also explains why the number of days since the new or full moon is more important for surface densities than clusters as they could be effectively redistributed as tides as they can redistribute clusters at depth.

Width was also considered to be an important factor for both clusters and surface densities in the regression trees with higher predicted abundances at wider beaches. Wider beaches may support higher abundances because they may not be completely

inundated during spring tides allowing large numbers of HSCs to spawn on the beach and lay clusters in burrows, while simultaneously allowing large numbers of eggs to accumulate on the beach surface (Jackson, et al., 2020). Wider beaches in the Southern region were observed to host the larger numbers of both clusters and surface densities at Cooks Beach, Highs Beach, and North Reeds Beach, while the lowest abundances were seen at Cape Shore Lab which was measured to have the smallest width in the region. Similar patterns were reflected in the other regions, however it was the most distinct in the Southern region due to the number of beaches and variety of widths.

Similar to the classification trees low SSTs were observed to predict low abundances of HSC egg clusters and surface densities as seen in Figure 26a and 26b, particularly when SSTs were below 15° C on the day of sampling. Low abundances of clusters were also observed when the five-day moving average reached 21° C and even lower when the SSTs on the day of sampling reached 21° C. Although this was not observed in the regression tree for surface egg densities, it was most likely due to the early cessation of sampling for surface densities as it is expected that they would also exhibit a similar issue with high SST as it continues to increase throughout the month of June and into July.

Geographic patterns concerning abundance of HSC egg clusters and surface densities were also detected in both regression trees. In the regression tree for HSC egg clusters, Figure 26a, the Northern and Central regions were predicted to have a reduced cluster abundance of 0.2 compared to the Southern region with 0.88. This was also reflected in the regression tree for surface density, observed in Figure 26, with a log normalized surface density of 3.1 in the Northern region and 3.6 in the Central and

Southern regions. This may be due to temperatures in these regions becoming less suitable for spawning as SSTs are higher in the Northern and Central regions earlier in the spawning season, lower salinity due to freshwater input from the Delaware River, or potentially other factors not identified in this analysis.

Although lunar cycles were identified as playing an important role in determining when HSCs begin spawning and lay their clusters in burrows, there is some suggestion that it may play a more important role in determining surface densities. Higher tides are associated with the full or new moon allowing wave propagation on beaches to be more extensive, allowing HSC clusters to be brought from their burrows to the surface. As wave action continues to rework coastal sediments, eggs can be carried along ocean currents depositing them in different locations – on or beyond their beach of origin.

Some factors not included in the CART models that would be advantageous in future work would be to include additional information on physical characteristics at each beach including sediment sizes, wave heights, and more specific information concerning storm events. HSCs prefer to spawn on beaches that contain coarser sediments compared to more fine sediments as it is easier to dig their burrows to lay their egg clusters (Brockman, 1990; Smith, et al., 2011; Smith, et al., 2017). Wave heights are recorded at several buoys operated by NOAA, however they do not provide information for specific beaches discussed in this analysis. By incorporating the use of sensors on individual beaches to record wave heights, such as a pressure transducer used in Jakson *et al.* (2020), would allow wave heights to be better understood during the spawning season. Interpolation methodologies could also be used to identify wave heights from the buoys, however not all buoys are operational at the same time due to mechanical malfunctions or

potential discontinuation of a specific buoy for maintenance or other factors. In this analysis information concerning storm events was not utilized, particularly the number of days since a major storm event. Because HSCs delay spawning during these time periods, understanding when these events occur that could delay spawning would be helpful to more precisely identify how the peak spawning periods may be impacted by such events – specifically the number of days since these events occurred.

HSC and Red Knots – Ecological Mismatch and Resiliency

Based upon this work HSC spawning and the arrival of the red knots currently align based upon the collected sampling data between 2015 and 2019 and determined using the CART analysis. Each region also displays increasing trends in both egg cluster abundances and surface densities, however they are not significant. Despite no significant trends, these observations agree with Niles *et al.* (2009) and Smith *et al.* (2017) that the HSC spawning population in the Bayshore area are either stable or increasing. This is a good sign for both red knots and HSC populations as they are stabilizing after significant population declines in the late 1990s and early 2000s (Niles, et al., 2009; McGowan, et al., 2011; Zimmerman, et al., 2016; Breese, 2017; Smith, et al., 2017; Atlantic States Marine Fisheries Commission, 2019).

Despite the stability or potential increase in the spawning HSC population in the Delaware Bay, there is a concern that HSCs could begin to spawn earlier in the year in response to warmer ocean temperatures. As SSTs in all regions reach the 17° C threshold that signals when peak HSC spawning occurs earlier than in the past, there is the potential for HSCs to advance when they spawn – between 12 to 18 days depending upon the

beach observed in Table 8. This advancement could cause peak egg abundances to emerge earlier in the season, potentially decreasing the available HSC eggs at the end of May resulting in further decreases in the red knot population. Although the degree of this impact could be lessened in some years due to the presence of stormy weather such as in 2017, the observed trend in the long-term could be disastrous for red knot populations if this advancement occurs more frequently – such as the timing of peak surface densities is 2018.

A secondary issue could assist with the development of this ecological mismatch is the aging female HSC population due to the moratorium on their harvests in the Bayshore area. It has been observed using telemetry data that older females begin spawning earlier than younger ones, and may contribute disproportionately to egg abundances when red knots are foraging in the area (Smith, et al., 2010). If older females shift their spawning behavior to met the advancing temperature threshold a possibility does exist that fewer high egg density locations could exist if younger spawning females have not reached sexual maturity. Future work on spawning HSCs in the Bayshore area should take on age demographics to better understand this potential change as it relates to migratory shore birds such as the red knot.

Despite spawning temperature threshold advancement and demographic dynamics for HSCs, efforts to improve the physical environment of the Bayshore area can be prioritized based upon the importance of physical characteristics identified in the regression trees such as beach width and sand depth – as seen in Figures 25 and 26. Sand depth and beach width are two physical parameters that can be improved upon with beach nourishment activities on Bayshore beaches to ensure the entire beach is not inundated

during spawning events and prevent females digging burrows from encountering mud and peat that could deleteriously influence egg development. Nourishment activities should focus on ensuring sand depths are greater than 40 cm and a beach width exceeding 22 m as they were predicted in the regression trees to increase cluster abundances observed in Figure 26a. These efforts should focus on increasing cluster abundances because HSCs lay their eggs as clusters in burrows and are then brought to the surface, potentially encouraging females to lay more clusters during the spawning season. Although other factors should also be considered such as sediment grain sizes and morphology, the specific importance on how it impacts abundance was not determined in this study

Beach nourishment activities have occurred several times in the Bayshore area, particularly in the Southern region in 2013 after Hurricane Sandy made landfall in 2012. Many of these beaches experienced widespread erosion and were littered with debris that could have increased HSC stranding causing higher mortality rates. Disaster relief funds were utilized for debris removal and beach nourishment between 2013 and 2016 resulting in habitat improvements in the most important region for HSC spawning (Smith, et al., 2020). Although these observations are encouraging, beach nourishment must continue prior to large scale disturbances like Hurricane Sandy to ensure habitat suitability persists.

Other slow changes can be just as damaging to this key stopover location overtime, such as sea-level rise (SLR). Although not focused on in this study, SLR can further increase erosion and is noted as an issue in the Bayshore area (Partnership of the Delaware Estuary, 2017). As SLR continues in the Bayshore area removing sediments

from the beaches, they could experience a decrease in both sand depth and beach width degrading the habitat making it less suitable for spawning. Another issue in the Bayshore area is increased urbanization that increases usage of the beaches in the area, specifically Cumberland County that has the highest urbanization rates and located in the Southern region (Partnership of the Delaware Estuary, 2017). Beach nourishment would assist in mitigating the rapid erosion of these sediments, while simultaneously increasing coastal protections for this growing community.

These efforts will assist in helping the horseshoe crab spawning population in the area and increase surface egg densities to the levels observed in the 1980's and early 1990's (Niles, et al., 2009), but these improvements met not be sufficient enough to protect the red knot as climate change continues to threaten other ecological stopover locations, their breeding grounds, and wintering locations. These compounding impacts could increase the frequency of disturbances to increase – mismatch between resources being one of them – resulting in further population declines like other long distance migrants as noted by Jones & Cresswell (2010) and McGowan et al. (2011). Despite the bleak outlook for red knots, this may not be the case for HSCs. Due to their wide spawning range and genetic diversity that shows some degree if variation that allows them to cope with varying temperatures geographically (Watson III, et al., 2016; Smith, et al., 2017), hope remains that the population could recover given more standardized population surveys throughout their spawning habitat that is compatible with those conducted in the Delaware Bay.

Continual improvements in the Bayshore area from natural and anthropogenic will assist the vital ecosystems that support both HSCs and red knots will be important as

they experience changes in the physical environment from climate change. As physical parameters change such as SSTs discussed at length along with others including but not limited to sea-level rise and coastal erosion inundate and remove the sandy beaches needed for HSCs to spawn, they may be unable to effectively respond decreasing their ability to respond to disturbances decreasing the resilience of the ecosystem as a whole. Although eggs are present in high abundances they still do not meet their observed abundance in the early 1990s (Niles, et al., 2009). Although management and monitorization are assisting with stabilizing the HSC population for the threatened red knot, consistent work must continue to ensure that the physical setting remains suitable for large-scale HSC spawning due to climate change.

Conclusions

Although restrictions on HSC harvests appears to have stabilized the population from further decline, there is a concern that HSC may begin spawning earlier in response to warmer SSTs due to climate change, setting up an ecological mismatch affecting the role of Delaware Bay as a critical migratory bird stopover. Due to the limited spatial coverage provided by the existing network of NOAA monitoring buoys, SSTs could not be analyzed at specific HSC spawning beaches. This study has demonstrated how the MUR dataset can provide high spatial and temporal coverage for SST allowing finer scale spatial patterns and trends to be investigated. The Northern region beaches warm up more quickly and reach consistently higher temperatures as compared to beaches in the Southern region. This regional pattern was most likely caused by warm freshwater from the Delaware River emptying into the Northern region, while the influx of colder Atlantic Ocean water reduces SSTs in the Southern region.

Utilizing data provided by Smith *et al.* (2020) for HSC egg clusters and surface densities, the relationship between SST and metrics of HSC spawning as seen in Table 3 were analyzed to discern a temperature threshold for peak spawning and important physical characteristics to increase egg abundances. Results from the CART analysis for both HSC egg clusters and surface densities show that peak spawning occurs when SSTs reach 17° C, with clusters reaching their peak abundance on Julian day 150 (May 29) and surface densities between 149 and 156 (May 28 and June 5). This suggests that based upon observed spawning data between 2015 and 2019, the peak of the spawning period currently aligns with when red knots are in the Bayshore area (Tispoura & Burger, 1999; McGowan, et al., 2011). It is worth stating that HSC can alter their behavior for spawning

to be later in the year during periods of storm events such as in 2017, or advance them earlier in the year during warmer SSTs as in 2018.

The HSC egg clusters and surface density data showed that the highest abundances appeared in the Southern region with lower abundances' in the Northern and Central regions. Although clusters and surface densities decreased in more northern locations, surface densities were shown to be higher than expected in locations that had low cluster abundances – such as East Point. This is most likely due to the mobilization of HSC eggs as they become suspended by wave action and bioturbation from other spawning HSCs and are transported to other locations on the beach or other beaches in the Bayshore area. Although highest densities were observed in the southern region, this mobilization likely creates other locations of higher than expected throughout the Bayshore area that can be utilized by foraging red knots.

Analyzing the MUR dataset for the years 2003 to 2019, shows that the date at when individual beaches are reaching the 17° C SST threshold were observed to have advanced by 17.3, 14.7, and 12.8 days over this time period in the Northern, Central, and Southern regions respectively. The advancement was also seen in all 14 beaches observed in this analysis, however variation was seen around this timing based upon the geographic region that it is situated in. A concerning addendum to the potential advancement to the spawning of HSCs in this region is if older females begin to spawn earlier as well (Smith, et al., 2010). This potential 'double advancement' could potentially cause species like the red knot to completely miss the peak spawning period and significantly reduce the fitness and fecundity of the species leading to further population declines – decreasing their ability to respond to future disturbances.

SST was determined to be the most important variable in explaining when spawning in the Bayshore area occurs. The CART model results suggests that physical characteristics of beaches in the Bayshore area are imporant in determining suitability of beaches as spawning habitat. Because HSCs do not display fidelity to specific beaches between spawning years, improving the habitat quality for HSCs on Bayshore beaches can assist in increasing the abundance of both egg clusters and surface densities throughout the area. Two specific factors that can improve spawning habitat are increasing the width of existing beaches and increasing the depth of sand. Increasing the beach width can assist with preventing the entire beach to become inundated during high tides or spring tide, allowing more HSCs to utilize these beaches during spawning events to increase the average number of clusters.

Results from the regression tree suggests that nourishment activities in the area should focus on sand depths being at least 40 cm deep and widths of at least 22 m. These recommendations are specifically targeted to increase clusters as HSCs deposit them in burrows on Bayshore beaches and would assist in increasing surface densities as they are mobilized and transport them throughout the Bayshoreare through bioturbation and wave action. Although these parameters can be met with Beach nourishment activities, they should also be done preemptively before disturbances occur. Observations have been made on the success of nourishment activities between 2013 and 2016 in the Southern (Smith, et al., 2020), but increasing the frequency of these initiatives improves the habitat quality for the spawning population of HSCs and protections for communities.

References

Alexander, D., 2013. Resilience and disaster risk reduction: an etymological journey. *Natural Hazards and Earth System Science,* pp. 2707-2716.

Atlantic States Marine Fisheries Commission, 2019. *2019 Horseshoe Crab Benchmark Stock Assessment Peer Review Report,* s.l.: Atlantic States Marine Fisheries Commission.

Bottom, M. L., Loveland, R. E. & Jacobson, T. R., 1988. Beach erosion and geochemical factors: Influence on spawning success of horseshoe crabs (Limulus polyphemus) in Delaware Bay. *Marine Biology,* Volume 99, pp. 325-332.

Breese, G., 2017. *"Chapter 6.7 - Horseshoe Crabs" in the Technical Report for the Delaware Estuary and Basin,* s.l.: Partnership for the Delaware Estuary and Basin.

Brockman, H. J., 1990. Mating behavior of horseshoe crabs, Limulus polyphemus. *Behaviour,* Volume 114, pp. 206-220.

Chabot, C. C. & Watson, W. H., 2010. Circatidal Rhythms of Locomotion in the American Horseshoe Crab Limulus polyphemus: Underlying Mechanisms and Cues that Influence Them. *Current Zoology,* pp. 499-517.

Chazdon, R. L., 2008. Beyond deforestation: Restoring forests and ecosystem services on degraded lands. *Science,* pp. 1458-1460.

Cheng, H., Chabot, C. & Watson III, W. H., 2016. Influence of Environmental Factors on Spawning of the American Horseshoe Crab (Limulus polyphemus) in the Great Bay Estuary, New Hampshire, USA. *Estuaries and Coasts,* pp. 1142-1153.

Chin, T. M., Vazquez-Cuervo, J. & Armstrong, E. M., 2014. On "Gridless" Interpolation and Subgrid Data Density. *Journal of Atmospheric and Ocean Technology,* pp. 1642-1652.

Chin, T. M., Vazquez-Cuervo, J. & Armstrong, E. M., 2017. A Multi-scale High-resolution Analysis of Global Sea Surface Temperature. *Remote Sensing of Environment,* pp. 154-169.

Church, J. A. & White, N. J., 2006. A 20th century acceleration in global sea-level rise. *Geophysical Research Letters,* pp. 1-4.

Cushing, D. H., 1969. The regularity of the spawning season of some fish. *Journal of Marine Science,* 33(1), pp. 81-92.

De' ath, G. & Fabricius, K., 2000. Classification and regression trees: A powerful yet simple technique for ecological data analysis. *Ecology,* 81(11), pp. 3178-3192.

Defeo, O. et al., 2009. Threats to sandy beach ecosystems: A review. *Estuarine, Coastal and Shelf Science,* Issue 81, pp. 1-12.

Durant, J. M., Herman, D. O., Ottersen, G. & Stenseth, N. C., 2007. Climate and the match or mismatch between predator requirements and resource availability. *Climate Research,* pp. 271-283.

Durant, J. M. et al., 2005. Timing and abundance as key mechanisms affecting trophic interactions in variable environments. *Ecology Letters,* pp. 952-958.

Ernstson, H. et al., 2010. Urban transitions: on urbandominated systems and human-dominated ecosystems. *A Journal of the Human Environment,* pp. 531-545.

Finchman, J. I., Rijnsdord, A. D. & Engelhard, G. H., 2013. Shifts in the timing of spawning in sole linked to warming sea temperatures. *Journal of Sea Research,* Volume 75, pp. 69-76.

Fisher, J. & Mustard, J. F., 2004. High Spatial Resolution Sea Surface Temperature from Landsat Thermal Infrared Data. *Remote Sensing and Environment* , pp. 293-307.

French, K., 1979. Laboratory culture of embryonic and juvenile Limulus. *Progress in Clinical and Biomedical Researcg,* Volume 29, pp. 61-71.

Gehrels, W. R., 1994. Determining relative sea-level change from salt-Marsh foraminifera and plant zoneson the coast of Maine, U.S.A. *Journal of Coastal Research,* pp. 990-1009.

Gunderson, L. H., 2000. Ecological resilience - in theory and application. *Annual Review of Ecology and Systematics,* pp. 425-439.

Haines, S. L., Jedlovec, G. J. & Lazarus, S. M., 2007. A MODIS sea surface temperature composite for regional applications. *IEEE Transactions on Geoscience and Remote Sensing,* 45(9), pp. 2919-2927.

Hale, R. L., Grimm, N. B., Vörösmarty, C. J. & Fekete, B., 2015. Nitrogen and phosphorous fluxes from watersheds of the northeast US from 1930 to 2000: Role of anthropogenic nutrient inputs, infrastructure, and runoff. *Global Biogeochemical Cycles* , pp. 341-356.

He, Q. & Silliman, B. R., 2019. Climate change, human impacts, and coastal ecosystems in the Anthropocene. *Current Biology, 29 (19),* pp. 1021-1035.

Holling, C. S., 1973. Resilience and stability of ecological systems. *Annual Review of Ecology and Systematica,* pp. 1-23.

Jackson, N. L., 1995. Wind and waves: Influence of local and non-local waves on mesoscale beach behavior in esruarine environments. *Annals of the Association of Geographers,* pp. 21-37.

Jackson, N. L., Nordstrom, K. F., Eliot, I. & Gerhard, M., 2002. 'Low energy' sandy beaches in marine and estuarine environments: A review. *Geomorphology,* Volume 48, pp. 147-162.

Jackson, N. L., Saini, S., Smith, D. R. & Nordstrom, K. F., 2020. Egg exhumation and transport on a foreshore under wave and swash action. *Estuaries and Coasts,* pp. 286-297.

Jones, T. & Cresswell, W., 2010. The phenology mismatch hypothesis: Are declines of migrating birds linked to uneven global climate change?. *Journal of Animal Ecology,* pp. 98-108.

Kent, E. C., Kennedy, J. J., Berry, D. I. & Smith, R. O., 2010. Effects of instrumentation changes on sea surface temperature measured in situ. *WIREs Climate Change,* pp. 718-728.

Lathrop, R. G., Allen, M. & Love, A., 2006. *Mapping and assessment of critical horseshoe crab spawning habitat in the Delaware Bay,* New Brunswick, NJ: Center for Remote Sensing and Spatial Analysis Rutgers University .

Lathrop, R. G. et al., 2013. *Mapping of Critical Horseshoe Crab Spawning Habitats of Delaware Bay,* New Brunswick, NJ: Walton Center for Remote Sensing and Spatial Analysis Rutgers University.

Lazarus, E. D., Ellis, M. A., Murray, A. B. & Hall, D. M., 2016. An evolving research agenda for human-coastal systems. *Geomorphology 256,* pp. 81-90.

Lüthi, D. et al., 2008. High-reolution Carbon Dioxide Concentration Record 650,000 to 800,000 Years before Present. *Nature,* pp. 379-382.

McGowan, C. P. et al., 2011. Demographic consequences of migratory stopover: Linking red knot survival to horseshoe crab spawning abundance. *Ecosphere,* pp. 1-22.

Miller, K. G. et al., 2013. A geological perspective on sea-level rise and its impacts along the U.S. mid-Atlantic Coast. *Earths Future,* Issue 1, pp. 3-18.

Nicholls, R. J., 2011. Planning for them impacts of sea level rise. *Oceanography* , pp. 144-157.

Niles, L. J. et al., 2009. Effects of horseshoe crab harvests in Delaware Bay on red knots: Are harvest restrictions working?. *BioScience,* 59(2), pp. 153-164.

NOAA, 2020. *NOAA National Centers for Environmental Information.* [Online]
Available at: https://www.ncdc.noaa.gov/cag/regional/time-series/101/pcp/12/3/1895-2020?base_prd=true&begbaseyear=1901&endbaseyear=2000&trend=true&trend_base=10&begtrendyear=1895&endtrendyear=2020

Okuro, A., Kubota, M., Tomita, H. & Hihara, T., 2014. Inter-comparisons of Various Global Sea Surface Temperature Products. *International Journal of Remote Sensing,* 35(14), pp. 5394-5410.

Partnership of the Delaware Estuary, 2017. *Technical Report for the Delaware Estuary and Basin,* s.l.: s.n.

Piao, S. et al., 2019. Plant phenology and global climate change: Current progress and challenges. *Global Change Biology,* Volume 25, pp. 1922-1940.

Robinson, Dave, 2018. *Warm and wet May, and an action packed Spring: May 2018 summary and a Spring recap.* [Online]
Available at: https://www.njweather.org/content/warm-and-wet-may-and-action-packed-spring-may-2018-summary-and-spring-recap
[Accessed 20 8 2020].

Robinson, D., 2017. *Talk of Drought Evaporates: May and Spring 2017 will Recaps.* [Online]
Available at: https://www.njweather.org/content/talk-drought-evaporates-may-and-spring-2017-recaps#:~:text=The%2018th%20was%20the%20warmest,at%20Fortescue%20to%2079%C2%B0.
[Accessed 20 8 2020].

Saba, V. S. et al., 2016. Enhanced warming of the Northwest Atlantic Ocean underclimate change. *Journal of Geophysical Research: Oceans* , 121(1), pp. 118-132.

Sánchez-Arcilla, A., García-Leòn, M., Gracia, V. & Devoy, R., 2016. Managing coastal environments under climate change: Pathways to adoption. *Science of the Total Environment,* Issue 572, pp. 1336-1352.

Sekiguchi, K. & Shuster, C. N., 2009. Limits on the Global Distribution of Horseshoe Crabs (Limulacea): Lessons Learned from Two Lifetimes of Observations: Asia and America. In: *Biology and Conservation of Horseshoe Crabs.* New York: Springer , pp. 5-24.

Shuster, C. N., 2015. The Delaware Bay Area, U.S.A.: A Unique Habitat of the American Horseshoe Crab Limulus polyphemus. In: *Changing Global Perspectives on Horseshoe Crab Biology, Conservation, and Management.* s.l.:Springer International Publishing, pp. 15-40.

Smith, D., Jackson, N. L., Nordstrom, K. F. & Weber, R. G., 2011. Beach characteristics mitigate the effects of onshore wind on horseshoe crab spawning: implications for matching with shorebird migration in Delaware Bay. *Animal Conservation,* pp. 575-584.

Smith, D. R. et al., 2017. Conservation status of the American horseshoe crab, (Limulus polyphemus): Regional assessment. *Rev Fish Biol Fisheries,* pp. 135-175.

Smith, D. R., Brousseau, L. J., Mandt, M. T. & Millard, M. J., 2010. Age and sex timing, frequency, and spatial distribution of horseshoe crab spawning in Delaware Bay: Insights from a large-scale telemetry array. *Current Zoology,* pp. 563-574.

Smith, D. R. & Michels, S. F., 2006. Seeing the elephant: Importance of spatial and temporal coverage in a large-scale volunteer-based programs to monitor horseshoe crabs. *Fisheries,* 31(10), pp. 485-491.

Smith, D. R. et al., 2002. Horseshoe crab (Limulus polyphemus) reproductive activity on Delaware Bay beaches: Interactions with beach characteristics. *Journal of Coastal Research,* 18(4), pp. 730-740.

Smith, J. A. M., Niles, L. J., Hafner, S. & Modjeski, D., 2020. Beach restoration improves habitat quality for American horseshoe crabs and shorebirds in the Delaware Bay, USA. *Marine Ecology Press Series,* Issue 645, pp. 91-107.

Smith, S. L., Cunniff, S. E., Peyronnin, N. S. & Kritzer, J. P., 2018. Prioritizing coastal ecosystem stressors in the Northeastern United States under increasing climate change. *Environmental Science and Policy,* Volume 78, pp. 49-57.

Solomon, S., Plattner, G.-K., Knutti, R. & Friedlingstein, P., 2009. Irreversible Climate Change Due to Carbon Dioxide Emissions. *PNAS,* pp. 1704-1709.

Spalding, M. D. et al., 2014. The role of ecosystems in coastal protection: Adapting to climate change and coastal hazards. *Ocean & Coastal Management 90,* pp. 50-57.

Swan, B. L., Hall, W. & Schuster, C. N., 2012. *The 2012 Delaware Bay Horseshoe Crab Spawning Survey,* s.l.: DNREC Alpha.

Tagliapietra, D., Sigovini, M. & Ghirardini, A. V., 2009. A review of terms and definitions to catagorise estuaries, lagoons and associated environments. *Marine and Freshwater Research,* 60(6), pp. 497-509.

Thomas, A. C. et al., 2017. Seasonal trends in and phenology shifts in sea surface temperature on the North American northeastern continental shelf. *Elementa Science of the Anthropocene,* 5(48), pp. 1-17.

Tispoura, N. & Burger, J., 1999. Shorebird diet during spring migration stopover on Delaware Bay. *The Condor,* Volume 101, pp. 635-644.

Tucker, A. M. et al., 2019. Foraging ecology mediates response to ecological mismatch during migratory stopover. *Ecosphere,* 10(10), pp. 1-17.

U.S. Fish and Wildlife Service, 2014. *Rufa Red Knot Background Information and Threats Assessment,* Pleasantville, New Jersey: s.n.

U.S. Fish and Wildlife Service, 2019. *Northeast Region Conserving the Nature of America.* [Online]
Available at: Fws.gov/northeast/red-knot/

Watson III, W. H., Johnson, S. K., Whitworth, C. D. & Chabot, C. C., 2016. Rhythms of Locomotion and Seasonal Changes in Activity Expressed by Horseshoe Crabs in their Natural Habitat. *Marine Ecology Progress Series, 542,* pp. 109-121.

Zimmerman, J., Hale, E., Smith, D. & Bennett, S., 2016. *Horseshoe crab spawning activity in Delaware Bay: 1999-2018,* s.l.: Atlantic States Marine Fisheries Commission's Horseshoe Crab Technical Committee .